ELSEVIER

Biophysical and Biochemical Sources of Variability in Canopy Reflectance

*Gregory P. Asner**

Analyses of various biophysical and biochemical factors affecting plant canopy reflectance have been carried out over the past few decades, yet the relative importance of these factors has not been adequately addressed. A combination of field and modeling techniques were used to quantify the relative contribution of leaf, stem, and litter optical properties (incorporating known variation in foliar biochemical properties) and canopy structural attributes to nadir-viewed vegetation reflectance data. Variability in tissue optical properties was wavelength-dependent. For green foliage, the lowest variation was in the visible (VIS) spectral region and the highest in the near-infrared (NIR). For standing litter material, minimum variation occurred in the VIS/NIR, while the largest differences were observed in the shortwave-IR (SWIR). Woody stem material showed opposite trends, with lowest variation in the SWIR and highest in the NIR. Leaf area index (LAI) and leaf angle distribution (LAD) were the dominant controls on canopy reflectance data with the exception of soil reflectance and vegetation cover in sparse canopies. Leaf optical properties (and thus foliar chemistry) were expressed most directly at the canopy level in the NIR, but LAI and LAD strongly controlled the relationship between leaf and canopy spectral characteristics. Stem material played a small but significant role in determining canopy reflectance in woody plant canopies, especially those with LAI<5.0. Standing litter significantly affected the reflectance characteristics of grassland canopies; small increases in the percentage of standing litter had a disproportionately large affect on canopy reflectance. The structural attributes of ecosystems determine the relative contribution of tissue, canopy, and landscape factors that drive variation in a reflectance signal. Deconvolution of these factors requires an understanding of the sources of variance at each scale (which is ecosystem dependent) as well as an adequate sampling (spectral, angular, and temporal) of the shortwave (400–2500 nm) spectrum.

INTRODUCTION

During the past several decades, the tools for vegetation remote sensing have evolved significantly. Optical remote sensing has expanded from the use of panchromatic and multispectral sensors to off-nadir looking instruments and imaging spectrometers. Ecological remote sensing now encompasses a wide range of applications including vegetation mapping, land-cover change detection, disturbance monitoring, and the estimation of biophysical and biochemical attributes of ecosystems (Asner et al., 1998a). As increased value has been placed on remote sensing for ecological research, management and modeling, a concomitant increase in understanding the factors that influence vegetation radiometric signals has been only partially realized.

Based on experimental and modeling evidence, vegetation reflectance is known to be primarily a function of tissue (leaf, woody stem, and standing litter) optical properties, canopy biophysical attributes (e.g., leaf and stem area, leaf and stem orientation, and foliage clumping), soil reflectance, illumination conditions, and viewing geometry (e.g., Ross, 1981; Goel, 1988; Myneni et al., 1989; Jacquemoud et al., 1992). Foliage and nonphotosynthetic vegetation (NPV=woody stems, standing litter, etc.) affect the radiation field through their reflectance and transmittance characteristics (Ross, 1981; Asner et al., 1998b). Leaf optical properties are a function of leaf structure, water content, and the concentration of biochemicals (Gates et al., 1965; Thomas et al., 1971; Wessman, 1990; Walter-Shea and Norman, 1991; Curran et al., 1992; Fourty et al.,

* Cooperative Institute for Research in Environmental Sciences, University of Colorado, Boulder

Address correspondence to Gregory P. Asner, Univ. of Colorado, CIRES/CSES, Campus Box 216, Boulder, CO 80309-0216. E-mail: asner@cses.colorado.edu

Received 27 October 1997; revised 13 February 1998.

REMOTE SENS. ENVIRON. 64:234–253 (1998)

655 Avenue of the Americas, New York, NY 10010

0034-4257/98/$19.00
PII S0034-4257(98)00014-5

1996). Plant structural attributes drive variation in canopy reflectance characteristics by orienting the scatterers (leaves and stems) in three-dimensional space, providing a means for photons to interact with multiple surfaces such as leaves, woody material, and soils.

Various biochemical (e.g., foliar lignin and nitrogen) and biophysical factors influencing canopy reflectance signatures have been studied in previous work (e.g., Goward and Huemmrich, 1992; Jacquemoud, 1993; Baret et al., 1994; Kupiec and Curran, 1995). Many efforts to better understand the role of these factors in controlling multispectral vegetation indices [e.g., NDVI (normalized difference vegetation index)] have improved their interpretation and uncovered important limitations and caveats (e.g., Huete, 1988; Asrar et al., 1992; Gamon et al., 1995; van Leeuwen and Huete, 1996; Huemmrich and Goward, 1997). To date, no studies have quantified the relative importance of each scale-dependent attribute that determines canopy reflectance across the shortwave (400–2500 nm) spectrum; the contribution of each factor relative to all other factors has not been adequately addressed. Yet, it is the interaction of these factors, including their potential covariance or unique behavior, that must be understood if advances in ecological remote sensing are to be achieved. Moreover, only a few studies have addressed the importance of NPV in canopy reflectance data (e.g., van Leeuwen and Huete, 1996; Huemmrich and Goward, 1997), yet woody stems and standing litter comprise a substantial portion of the canopy in many ecosystems such as grasslands, shrublands, savannas, and dry woodlands. Our ability to both interpret remotely sensed optical data and develop new vegetation remote sensing approaches hinges directly on our ability to resolve the multitude of factors controlling canopy and landscape reflectance signatures.

Recent work has demonstrated that horizontal mixing of vegetation types or materials across the landscape is primarily a linear process (Roberts et al., 1993). Based on this linear mixing assumption, the relative cover of plant canopies and bare soils patches can be separated with reasonable accuracy (Adams et al., 1995; Wessman et al., 1997). In such analyses, the endmembers tend to represent vegetation types which, in turn, represent biochemically and structurally complex entities, each with attributes that make them spectrally distinct from one another. While the horizontal extent of covers can be adequately determined from a linear mixing perspective, the interaction of photons with vegetation components in vertical space is known to be highly nonlinear (e.g., Ross, 1981; Myneni et al., 1989; Borel and Gerstl, 1994; Asner and Wessman, 1997). This nonlinearity in volumetric mixing (e.g., canopies with increasing leaf area) makes it extremely difficult to study the role of tissue and structural attributes that determine canopy and landscape radiative characteristics using field measurements alone. Conversely, analyses based solely on models without direct connection to field-measurable quantities can lead to erroneous conclusions if the realistic range of model parameter values is not known.

Imaging spectrometry is a unique type of optical remote sensing because the surface radiance is sampled in contiguous, narrow spectral bands. Multispectral instruments such as the Landsat Thematic Mapper (TM) convolve large, noncontiguous regions of the spectrum into broad bands, and thus, a single number represents the radiometric dynamics of a large region of the spectrum. Imaging spectrometers, such as the Airborne Visible and Infrared Imaging Spectrometer (AVIRIS), acquire radiance information in <10 nm bandwidths from roughly 400 nm to 2500 nm, providing a capability to analyze the surface by absorption feature or by the shape of the reflectance continuum. Imaging spectrometer data thus provide a convenient spectral framework in which to explore the relative contribution of tissue, canopy, and landscape attributes to both of these optical remote sensing characteristics.

In this article, a combination of field and modeling techniques is used to quantify the relative contribution of leaf, woody stem, and litter optical properties and canopy structural attributes to vegetation reflectance data. In contrast to recent studies focused on scaling leaf biochemical properties to the canopy level (Jacquemoud et al., 1995), this study approaches the scaling problem from the observed variability in tissue optical properties resulting from an established range of biochemical conditions, and then examines the importance of this tissue versus canopy structural variability at landscape scales using a plant canopy radiative transfer model. There were three specific objectives of this work: 1) Determine the variability in leaf, woody stem, and standing litter reflectance and transmittance properties across a wide array of plant species, genera, growthforms, lifeforms, and functional groups along a strong climatic gradient and across a broad range of foliar biochemistry. 2) Determine the spectral regions in which tissue optical characteristics most significantly influence canopy reflectance data. 3) Test the relative importance of tissue optical, canopy structural, and soil reflectance variability in driving changes in landscape (pixel-level) reflectance for three specific ecosystem types: grasslands, shrublands, and broadleaf woodlands.

METHODS

Study Sites

A series of grassland, shrubland, savanna, and tropical woodland sites were selected in Colorado, New Mexico, and Texas and in the Cerrado region of Brazil to assess the optical variability of leaf, woody stem, and standing grass litter (Table 1). These sites provided access to a wide

Table 1. Foliar, Woody Stem, and Standing Litter Optical Samples and Soil Reflectance Samples Collected along an Ecosystem–Climatic Gradient Extending from Desert Shrublands of New Mexico, USA to Tropical Woodlands in Brazil[a]

Site Name	*Resource Area*	*Location (Latitude)*	*Annual PPT (mm)*	*Minimum MMT (°C)*	*Maximum MMT (°C)*	*Dominant Soil Type*	*Dominant Vegetation*
Jornada LTER	Chihuahuan Desert	32°31′N	230	13.1 (Jan.)	36.5 (Jun.)	Aridisols	Desert grassland/shrubland
Sevilleta LTER	Great Plains, Chihuahuan Desert, Great Basin Shrub-Steppe	34°15′N	255	−5.0 (Dec.)	33.0 (Jul.)	Entisols, vertisols	Mixed grassland shrubland-steppe
Colorado Springs	Front Range Woodland–Grassland Transition	38°49′N	402	−8.8 (Jan.)	29.2 (Jul.)	Aridisols, alfisols	Temperate woodland
Sonora	Edwards Plateau	30°10′N	575	9.0 (Jan.)	30.0 (Jul.)	Entisols, alfisols	Shrubland savanna
Vernon	Rolling Plains	33°57′N	640	−1.7 (Jan.)	35.8 (Jul.)	Mollisols, entisols	Temperate savanna grassland
La Copita	Rio Grande Plains	27°40′N	710	7.2 (Jan.)	35.4 (Aug.)	Ultisols, alfisols	Subtropical savanna parkland
Cerrado	Central Brazilian Plateau	15°56′S	1490	15.6 (Jul.)	26.6 (Mar.)	Oxisols	Tropical woodland/savanna

[a] PPT=precipitation; MMT=mean monthly temperature.

variety of species representing a diverse array of plant functional and structural types and tissue chemistry. The sites also represented a strong rainfall (ppt) gradient ranging from roughly 230 mm ppt yr^{-1} at the Jornada LTER desert shrubland site in southern New Mexico to almost 1500 mm ppt yr^{-1} at the Cerrado tropical woodland site (Table 1). Differences in mean monthly maximum and minimum temperature as well as soil type were also represented across this range of sites.

Tissue Optical Measurements

A comprehensive analysis of the characteristics and variability in leaf, woody stem, and standing litter optical properties across the Texas portion of the climate gradient was recently reported (Asner et al., 1998a; in press). A goal of the present study was to extend the Texas data set to include an even wider range of climate conditions, plant functional and structural groups, and foliar chemistry. The Brazilian Cerrado site was of particular interest because of its highly variable foliar chemistry; it is one of the most floristically diverse regions of Earth, with strong species-specific differences in foliar chemistry (Eiten, 1972; Stewart et al., 1992; Sprent et al., 1996). The total species composition of the combined data set is listed in Table 2, with 1440 samples (720 foliar, 720 litter+woody stem) representing 59 woody plant and 20 herbaceous species from at least 10 functional classifications.

At each site, leaves of woody species (trees, shrubs, and subshrubs) were sampled by clipping 5–10 branches from individual plants. Branches were placed in airtight polyethylene bags and stored in a cooler until the spectra were measured. Similarly, grass and standing litter samples were collected by placing whole grass clumps (including some roots and soil) into bags to maintain leaf moisture conditions. All measurements were subsequently conducted within 15 min of sample collection. Full-range hemispherical reflectance and transmittance values (400–2450 nm) were obtained using a spectroradiometer (Analytical Spectral Devices, Inc., Boulder, Colorado), a $BaSO_4$ integrating sphere (LI-1800, Licor Inc., Lincoln, Nebraska), and a light source modified for full-range spectral measurements. The ASD spectrometer acquires measurements in 1.4 nm intervals in the visible/near-IR [400–1300 nm; full-width at half-maximum (FWHM)=3–4 nm] and 2.2 nm in the shortwave IR region (FWHM=10–12 nm; 1300–2450 nm). Each reflectance and transmittance sample was a mean of 200 individual full-range spectral measurements.

A modified version of the Daughtry et al. (1989) method for spectral analyses of needle leaves was used for the leaflets of species not completely covering the sample port on the integrating sphere (e.g., *Acacia, Prosopis*, green and senescent grass leaves). Middleton et al. (1996) showed that this method for conifer needles contained a procedural error that could lead to apparent

Table 2. Species Represented in the Tissue Optical Properties Analysis from Seven Edaphically and Climatically Diverse Ecosystems in North and South America

Species[a]	*Site*[b]	*Attributes*[c]	*Species*[a]	*Site*[b]	*Attributes*[c]
*Acacia berlandieri**	3	W,C3,L,D	*Miconia albicans*	7	W,C3,EG,AI
*Acacia farnesiana**	3	W,C3,L,D	*Miconia falax*	7	W,C3,EG,AI
*Acacia greggii**	3	W,C3,L,D	*Miconia ferruginata*	7	W,C3,EG,S,AI
*Acacia rigidula**	3	W,C3,L,D	*Morus microphylla*	2	W,C3,D
Acer negundo	1,4	W,C3,D	*Neea theifera*	7	W,C3,D
Agropyron cristatum	2	H,C3	*Ouratea hexasperma*	7	W,C3,EG,S
Aristida capillacea	7	H,C4	*Palicourea coriacea*	7	W,C3,EG,S,AI
Aristida purpurea	1	H,C4	*Panicum decipens*	7	H,C4
Ascosmium dasycarpum	7	W,C3,L,EG	*Panicum maximum*	7	H,C4
Aspidosperma tomentosum	7	W,C3,D	*Paspalum* spp.	3	H,C4
Berberis trifoliolata	2	W,C3,EG	*Pisonia noxia*	7	W,C3,D
Blepharcalyx salicifoleus	7	W,C3,EG	*Plathymenia reticulata*	7	W,C3,L,N,D
Bothriochloa ischaemum	3	H,C4	*Populus augustifolia*	1,4	W,C3,D
*Bouteloua curtipendula**	2	H,C4	*Prosopis glandulosa*	1,2,3,5,6	W,C3,L,N,D
*Bouteloua eriopoda**	5,6	H,C4	*Prosopis sonora*	2	W,C3,L,D
*Bouteloua rigidiseta**	1	H,C4	*Qualea grandiflora*	7	W,C3,D,S,AI
Byrsonima crassa	7	W,C3,EG,S	*Qualea multiflora*	7	W,C3,D,AI
Caryocar brasiliense	7	W,C3,D	*Qualea parviflora*	7	W,C3,D,AI
Celtis reticulata	2	W,C3,D	*Quercus buckleyi*	1	W,C3,D
*Cenchrus ciliaris**	3,7	H,C4	*Quercus gambelii*	1,4	W,C3,D
Cercis canadensis	2	W,C3,L,D	*Quercus pungens*	2	W,C3,EG,S
Chloris pluriflora	3	H,C4	*Quercus virginiana*	2	W,C3,EG,S
Colubrina texensis	2	W,C3,D	*Rapanea guianensis*	7	W,C3,EG,S
Condalia hookeri	3	W,C3,D	*Roupala montana*	7	W,C3,EG,S
Connarus fulvus	7	W,C3	*Rhus aromatica*	4	W,C3
Dalbergia misculobium	7	W,C3,L,N,D	*Rhus microphylla**	2	W,C3
Didymopanax macrocarpum	7	W,C3,EG,S	*Schizachyrium scoparium*	2	H,C4
Diospyros texana	3	W,C3,D	*Schlerolobium paniculatum*	7	W,C3,L,EG
Enterolobium ellipticum	7	W,C3,L,D	*Sophora secundiflora*	2	W,C3,EG,S
*Erioneuron pilsoum**	2	H,C4	*Sorgastrum nutans**	2	H,C4
Erythroxylum suberosom	7	W,C3,EG,S	*Stipa leucotricha*	1	H,C3
Forestiera angustofolia	2	W,C3,D	*Stryphnodendron adstringens*	7	W,C3,L,D
*Hilaria belangeri**	2	H,C4	*Styrax ferrugineta*	7	W,C3,EG
Hymenea stigonocarpa	7	W,C3,L,D	*Trachypogon montufari*	7	H,C4
Kielmeyera coriacea	7	W,C3,D,S	*Tripsacum dactyloides*	2	H,C4
Larrea tridentata	5,6	W,C3,EG	*Ugnadia speciosa*	2	W,C3,D
Leucaena retusa	2	W,C3,L,D	*Vochysia elliptica*	7	W,C3,EG,S,AI
Lonicera albiflora	2	W,C3,D	*Vochysia thyrsoides*	7	W,C3,EG,S,AI
Mahonia trifoliolata	3	W,C3,EG,S	*Zanthoxylum fagara*	3	W,C3,EG-NS
Melinis minutiflora	7	H,C4			

[a] Some of the known functional attributes of each species are provided. $n=10$ per species unless an * indicates $n=5$.
[b] 1) Vernon, 2) Sonora, 3) La Copita, 4) Colorado Springs, 5) Sevilleta, 6) Jornada, 7) Cerrado.
[c] W=woody plant, H=herbaceous plant, D=deciduous, EG=evergreen, S=sclerophyll, L=legume, N=confirmed nitrogen fixer, Al=aluminum hyperaccumulator, C3=C_3 physiology, C4=C_4 physiology.

negative transmittance values when the gap fraction between needles in the sample port was too large. Suggestions provided by Middleton et al. (1996) and Mesarch et al. (in review) were used to decrease the gap fraction in the sample port to less than 10%, minimizing this problem in the measurements.

Woody stem material was collected from trees and shrubs by removing thin, opaque slices of the outer bark. Flat areas on the stems were selected to ensure that the sample port of the integrating sphere would close properly. Reflectance spectra were collected from 5–10 individual bark samples from each species, with each sample representing the mean of 200 spectral measurements.

Foliar Chemistry

Several key foliar constituents were analyzed to establish the range of biochemical attributes represented by the leaf optical properties data set. Woody plant and grass foliar carbon (C), nitrogen (N), lignin, cellulose, polar and nonpolar extractables, and fresh leaf water content were assessed. Polar extractables include soluble polyphenols, sugars, and starch, while nonpolar extractables represent fats, waxes, and nonsoluble phenolics. The foliar samples used in determining leaf optical properties were weighed fresh, oven dried at 70°C for 48 h, reweighed, and ground in a Cyclotec grinder with a #40 mesh filter. Leaf water content was determined by dif-

ference of the fresh and dried leaf weights. Total C and N content was analyzed using a Fisons EA1108 CHN Elemental Analyzer (Fisons Instruments, Inc., Beverly, Massachusetts). Foliar lignin, cellulose, and polar/nonpolar extractables were determined by wet chemistry separation using 100°C water and dichloromethane extractant (TAPPI, 1975; 1996). The residue was separated into acid-soluble (cellulose) and acid-insoluble (lignin) fractions using a two-stage digestion in sulfuric acid (Effland, 1977).

Soil Reflectance

Full spectral range (400–2450 nm) soil reflectance measurements were collected at each field site. A variety of soil types were sampled within one hour of solar noon (Table 1). The fiber optic of the spectrometer was held 1m above ground level in a nadir position (IFOV ~0.4 m), and care was taken to ensure that only bare soil was sampled. A white calibration panel (Spectralon, Labsphere, North Sutton, New Hampshire) was used to convert radiance values to reflectance. Soil reflectance measurements were also collected after rainfall events at the Texas and Brazil sites to capture the variability caused by soil wetting (Irons et al., 1992).

Radiative Transfer Modeling

While many canopy radiative transfer models have been developed in recent years, only a few can simulate the interaction of photons with multiple plant components (e.g., leaves, woody stems, and litter) within canopies. Those that can perform this task range in complexity from relatively simple but fast 2-stream models such as SAIL (Verhoef, 1984; Braswell et al., 1996) to complex three-dimensional photon transport models such as 3-D DISORD (Myneni and Asrar, 1993), which are considered the most accurate but computationally expensive. Because of the high computational requirement for simulating 220 AVIRIS bands (especially for the perturbation analyses to follow), SAIL was selected since it produces nadir reflectance values with reasonable accuracy (e.g., Major et al., 1992; Huemmrich and Goward, 1997). The model was restructured from its original formulation (Verhoef, 1984) to include multiple tissue components (Braswell et al., 1996), then further modified here for use with hyperspectral data. Wavelength-independent calculations (e.g., leaf angle distribution) are made only once per simulation, while those calculations requiring the leaf and NPV optical properties (e.g., multiple scattering) are iterated by wavelength.

The model produces top-of-canopy reflectance values from the following input parameters: leaf and NPV area index (LAI and NPVAI), leaf and NPV angle distributions (LAD and NPVAD), leaf and NPV hemispherical reflectance (ρ) and transmittance (τ) properties and soil reflectance ($\rho_{leaf}(\lambda)$, $\tau_{leaf}(\lambda)$, $\rho_{npv}(\lambda)$, $\tau_{npv}(\lambda)$, $\rho_{soil}(\lambda)$), Sun and view zenith and azimuth angles (θ_{sun},φ_{sun},θ_{view},φ_{view}), and a hot-spot parameter for each vegetation component (H_{leaf}, H_{npv}) (Kuusk, 1991):

$$R(\lambda)=f(\text{GEOMETRY, STRUCTURE, TISSUES, } \rho_{soil}(\lambda)), \quad (1)$$

where

$$\text{GEOMETRY}=(\theta_{sun}, \varphi_{sun}, \theta_{view}),$$
$$\text{STRUCTURE}=(\text{LAI, NPVAI, LAD, NPVAD}), \varphi_{view}, H_{leaf}, H_{npv},$$
$$\text{TISSUES}=(\rho_{leaf}(\lambda), \tau_{leaf}(\lambda), \rho_{npv}(\lambda), \tau_{npv}(\lambda)).$$

Scattering characteristics at the tissue and soil level are modeled as isotropic. Measured leaf, woody stem, litter, and soil spectra were convolved to the AVIRIS spectral response curves to produce 220 optical channels from 400–2450 nm. All analyses were subsequently based on the AVIRIS channels. LAI and NPVAI are given on a $m^2\ m^{-2}$ basis, and LAD and NPVAD are modeled as an ellipsoidal distribution with a mean leaf and NPV angle (Campbell, 1986). For analyses in this article, solar zenith and azimuth angles (θ_{sun}, φ_{sun}) were held constant at 30° and 0°, respectively. View zenith and azimuth angles (θ_{view}, φ_{view}) were both set to 0°.

Tissue vs. Canopy Structural Variability

Two standard deviations (s.d.) about the mean of leaf reflectance and transmittance (total range=4 s.d.) were used as the criterion to determine the role of leaf optical variation at canopy scales. Ratios of high/low canopy reflectance resulting from leaf optical variability were computed by wavelength to determine where foliar characteristics play the most significant role in driving spectral changes of plant canopies.

The impact of canopy structural attributes on canopy reflectance was tested by systematically changing LAI and LAD through their ecologically realistic range. Changes in various absorption features and the shape of the reflectance continuum were also evaluated by calculating first derivatives (approximated as finite differences) along each canopy reflectance spectrum (Wessman et al., 1989). The role of leaf optical variability was then assessed for each canopy structural scenario to uncover links between leaf and canopy spectral characteristics.

Four standard deviations in woody stem and standing litter optical properties (from the field data) were used to test their importance at canopy scales. Several LAI and LAD scenarios for tree and grass canopies were modeled using this range of measured NPV optical properties. Tree canopy simulations employed woody plant leaf and stem optical properties, while herbaceous canopies used grass leaf and standing litter optics. The ratio of leaf-to-stem area was selected from literature sources to ensure that the simulations realistically represented NPV.

Sources of Variability in Contrasting Biomes

The tissue- and canopy-level determinants of vegetation reflectance variability were assessed by combining the

field and modeling components of the study into several perturbation analyses. Simulations were conducted for three contrasting ecosystems: grasslands, shrublands, and broadleaf woodlands. The Konza and Jornada Long-term Ecological Research (LTER) sites were selected to represent the structural attributes of the grasslands and shrublands, respectively. The Cerrado site was chosen to represent broadleaf woodlands.

Tissue and soil optical properties and canopy structural attributes were randomly selected within a range defined for each ecosystem type, and a top-of-canopy reflectance spectrum was generated (called a base-case scenario). For every base-case scenario, each parameter was, in turn, perturbed by ±10% of its measured range, and the simulation repeated (10 parameters perturbed=10 repeated simulations following the base-case). The ±10% range was selected based on the notion that a smaller change in each variable would generally be undetectable using field methods. For example, a change in vegetation cover of less than 10% is difficult to verify via field or remote sensing measurements. Similarly, a change in LAI of less than 10% is not readily detectable since the error in measuring LAI in the field is typically of equal or greater order.

A database was created for all model simulations (n=1000 base case+1000×10 perturbed parameters= 11,000 AVIRIS reflectance simulations). The sum of the squares of differences, or merit-of-change value, between the original reflectance value at each wavelength and the value derived following each parameter perturbation was recorded. A principal components analysis (PCA) was then performed on the merit-of-change values at each wavelength. Since the first principal component axis represents the direction of maximum variance, the weighting of each perturbed parameter's contribution to that axis was a measure of the model's sensitivity to the perturbation at a given wavelength (Privette et al., 1994; Asner et al., in press). Thus, a sensitivity index was derived for all perturbed parameters at each wavelength, providing a test of the relative contribution of each scale-dependent tissue and structural variable to a pixel-level reflectance spectrum. The entire procedure was carried out for the grassland, shrubland, and woodland sites. Differences between ecosystems were evaluated to identify vegetation-specific limitations to the estimation of tissue optical and canopy structural variables using optical remote sensing.

RESULTS AND DISCUSSION

Variation in Foliar Chemistry

Foliar carbon (C) and nitrogen (N) chemistry results are summarized in Table 3. Among woody plants, lignin values ranged from 8.9% to 51.4%, while cellulose varied from 24.8% to 60.7%. These lignin and cellulose ranges exceed concentrations presented in other studies (e.g., Jacquemoud et al., 1996; Martin and Aber, 1997), primarily due to the sharply varying chemistry of the Cerrado species. In this region of Brazil, extreme soil nutrient impoverishment and high aluminum toxicity, coupled with high fire frequency, have resulted in a diverse range of phenological strategies among species (Eiten, 1972). In turn, lignin and cellulose content of Cerrado foliage varies widely, as these two C constituents play a major role in determining leaf morphology and longevity—two factors influencing phenology.

Grass lignin and cellulose concentrations were less variable than those of woody plants. Mean (±1 s.d.) lig-

Table 3. Foliar Carbon, Nitrogen, and Water Chemistry Results for All Woody Plant and Herbaceous Species Used in the Leaf Optical Properties Analysis

Foliar Attribute	*Mean % (±1 s.d.)*	*Min %*	*Max %*
Woody Plants			
Lignin	25.3 (9.9)	8.9	51.4
Cellulose	39.4 (8.0)	24.8	60.7
Polar extractables[a]	27.1 (7.9)	9.6	50.0
Non-polar extractables[b]	8.2 (3.1)	2.8	17.0
Total carbon (% DW)	48.1 (4.3)	37.8	52.7
Total nitrogen (% DW)	1.7 (1.3)	0.9	5.2
Total water (% FW)	49.2 (6.2)	37.2	63.1
Grasses			
Lingin	18.7 (3.4)	15.0	28.7
Cellulose	60.6 (1.9)	56.3	63.8
Polar extractables	14.8 (3.1)	6.1	18.5
Non-polar extractables	6.0 (1.6)	2.5	8.3
Total carbon	39.3 (2.1)	37.1	43.4
Total nitrogen	1.2 (0.4)	0.7	1.9
Total water	58.7 (3.6)	51.9	66.0

[a] Sugars, starch, soluble polyphenols.
[b] Fats, waxes, nonsoluble phenolics.
FW=fresh weight; DW=dry weight.

nin and cellulose context was 18.7% (3.4) and 60.6% (1.9), respectively. Grass lignin values were significantly lower than those of woody plants, while grass cellulose was higher than woody plant cellulose (student t-tests, $p<0.05$). The repeatedly high cellulose values were expected among grasses, as this C constituent tends to be relatively more abundant in grasses compared to woody plants (Bidlack and Buxton, 1992).

There was also a broad range of total C and N values among woody plants. In particular, the variation in N content reflects the wide array of species collected from soils of varying nutrient status as well as the presence of both N-fixers and nonfixers. Finally leaf water content varied significantly (Table 3), presumably due to differences in mesophyll structure, physiology, and stress. Overall, these results indicate that the subsequent analysis of leaf optical properties incorporates an extremely wide range of foliar C, N, and H_2O chemistry.

Variability in Tissue and Soil Optical Properties

The similarities and differences in tissue optical characteristics by species, genera, growthforms, lifeforms, or functional groups will not be covered in this article, as much of this discussion took place in Asner et al. (1998b; in press). Instead, the total variance in the optical properties of leaves, woody stems, and standing litter material will be defined (analogous to the biochemistry) to facilitate an analysis of their importance at canopy and landscape scales. A general discussion of the various absorption features in the spectra will be provided only to point out their significance at larger scales. Throughout the remainder of the article, the following spectral regions will be discussed: visible (VIS=400–700 nm), near-infrared (NIR=700–1300 nm), shortwave-IR from 1500–1900 nm (SWIR1), and shortwave-IR from 1900–2450 nm (SWIR2).

Mean (±1 s.d.) reflectance and transmittance properties of woody plant and grass leaves are shown in Figure 1. Woody species had consistently lower reflectance values than grass species throughout the VIS (t-tests at each wavelength, $p<0.05$), whereas woody species had higher values throughout the NIR (t-tests, $p<0.05$). There were no significant reflectance differences between woody plant and grass vegetation types in the SWIR. In comparing transmittance spectra, no significant differences were observed between the woody plant and grass groups (t-tests).

Among woody plants, the reflectance variability was lowest in the VIS (coefficient of variation=c.v.=11–14%), and highest in the SWIR2 (c.v.=20–28%) (Fig. 1a). Among grass species, the lowest reflectance variation was in the VIS (c.v.=6–9%), while the highest was in the NIR (c.v.=11–12%) (Fig. 1b). Transmittance variability among woody plant leaves was lowest in the NIR (c.v.=11–13%), and highest in the SWIR2 near 2200 nm (c.v.=33–45%). Grass species displayed similar trends with lowest variation in the NIR (c.v.=10–12%), and highest variation in the SWIR2 (c.v.=20–36%). Overall, transmittance variability

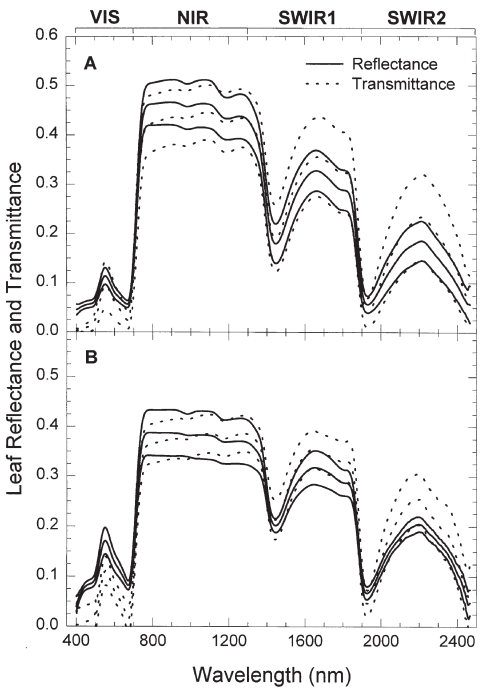

Figure 1. Mean (±1 s.d.) leaf hemispherical reflectance (solid lines) and transmittance (dotted lines) properties collected from sites in the United States and Brazil: A) woody plant species and B) herbaceous species. Major spectral regions discussed throughout the article are indicated: visible (VIS), near-infrared (NIR), and shortwave-infrared (SWIR1, SWIR2).

was greater than reflectance variability between 2000 nm and 2450 nm.

Relatively stable optical properties of leaves at VIS wavelengths are due to biochemical characteristics resulting from the presence of biologically active pigments (e.g., Gausman, 1982; Maas and Dunlap, 1989; Walter-Shea and Norman, 1991). Strong absorption features near 450 nm and 680 nm result from chlorophyll activity (Salisbury and Ross, 1969), while significant increases in reflectance and transmittance in the NIR result from photon scattering at the air–cell interfaces within the leaf spongy mesophyll (Woolley, 1971; Boyer et al., 1988). The two local absorption features on the NIR plateau (~1000 nm and 1200 nm) were most pronounced in the woody plants and are weak water absorption features (Gao and Goetz, 1995).

In the SWIR1 and SWIR2, leaf spectra are dominated by water absorption which obscures biochemical features related to lignin and other carbon constituents (Woolley, 1971; Fourty et al., 1996). The general shape of the reflectance continuum in the SWIR region can be simulated using glass beads immersed in water, since the refractive index of water and glass closely match that of cells in a water-filled leaf (Woolley, 1971; Wessman, 1990; Gao and Goetz, 1995). While it is well known that water content dominates NIR and SWIR leaf reflectance

and transmittance properties, quantification of the relative importance of water, carbon, and nitrogen continues to be difficult (Curran et al., 1992; Fourty et al., 1996).

Standing litter and woody stem optical properties were generally more variable compared to leaves (Fig. 2). Litter reflectance and transmittance c.v.'s were 8–35% (lowest in VIS, highest in SWIR2) and 23–51% (lowest in NIR, highest in SWIR2), respectively. These results were similar to those found for the Texas data set (Asner et al., 1998b). The wide-ranging litter optical values are primarily due to differences in residual water content as well as species-specific differences in carbon (e.g., lignin, cellulose) concentration (Murray and Williams, 1987; Asner, unpub. data).

Coefficients of variation for woody stem reflectance ranged from 20% to 45% (highest in NIR region near 900 nm, lowest in VIS). This high variability likely occurred from differences in surface moisture and carbon constituents of the outermost bark (Asner and Wessman, 1997); however; stem spectral–biochemical relationships have not been quantitatively established. In general, woody stem and litter spectra showed fewer water absorption features than green leaf material, allowing the features associated with lignin and other organic compounds (at roughly 1700 nm, 2000 nm, and 2200 nm) to emerge in the spectra (Curran et al., 1992; Verdebout et al., 1994; Jacquemoud et al., 1996).

Mean (±1 s.d.) soil reflectance is shown in Figure 3. Strong atmospheric absorption features centered near 1400 nm and 1900 nm were due to water vapor, preventing measurements and subsequent modeling of these spectral regions. Soil reflectance variability was highest in the SWIR2 (c.v.=18–20%) and lowest in the VIS (c.v.=14–16%).

Figure 2. A) Mean (±1 s.d.) standing litter reflectance (solid lines) and transmittance (dotted lines) properties collected from sites in the United States and Brazil; B) mean (±1 s.d.) woody stem reflectance.

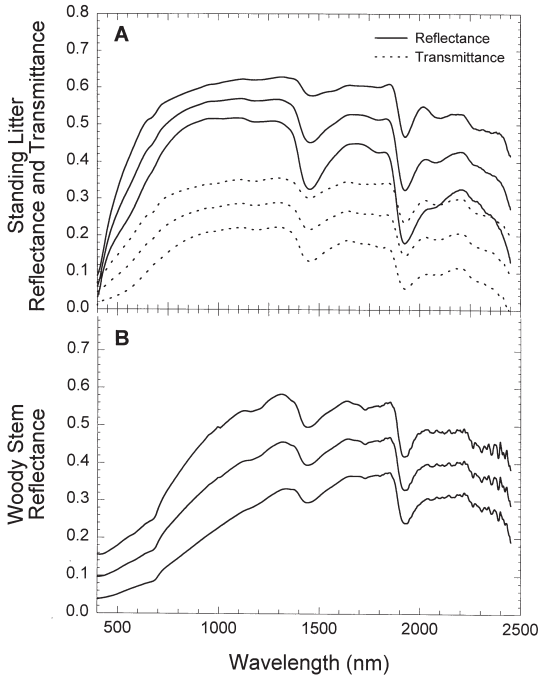

Leaf Optical Variability at Canopy Scales

For analyses in this and the following two sections, leaf and NPV optical properties were taken from Figures 1 and 2 unless noted otherwise. The darkest soil spectrum from the field data (Fig. 3) was used to better isolate the effects of changing leaf and canopy structural conditions (to minimize soil effects). Figure 4 shows the role of leaf optical variability (4 s.d. in Fig. 1) on nadir-viewed canopy reflectance as simulated for a canopy of low and high LAI (1.5 and 6.0). The former is a common LAI scenario for grasslands, while the latter is typical of forest canopies (Table 4). In the low LAI scenario, leaf optical variability played a relatively small role in driving canopy reflectance variation (Fig. 4a). The total range in canopy reflectance resulting from leaf optical variation was <1% in the VIS and a maximum of 4% in the NIR (Fig. 4c). At high canopy LAI, the effects of leaf optical variability were more pronounced, causing maximum variation in canopy reflectance in the NIR (14–18%; Fig. 4b). In the VIS and along the "red edge" (~700 nm), effects of leaf-level variation were still extremely small (<0.5%; Figs. 4b,c). Leaf effects at canopy scales were greater in the SWIR1 than in the SWIR2 because the single scattering albedo (reflectance+transmittance) of fresh green leaves is higher in the SWIR1.

Structural Effects on Canopy Reflectance Properties

Canopy LAI variation had a strong influence on reflectance signatures (Fig. 5a), with the most pronounced effect in the NIR and the smallest effect in the VIS region. Structure enhances canopy reflectance in spectral regions where the scatterers are "bright" (e.g., NIR for green

Figure 3. Mean (±1 s.d.) soil reflectance spectra collected at sites in the United States and Brazil. Strong atmospheric water absorption near 1400 nm and 1900 nm prevented measurements in those spectral regions.

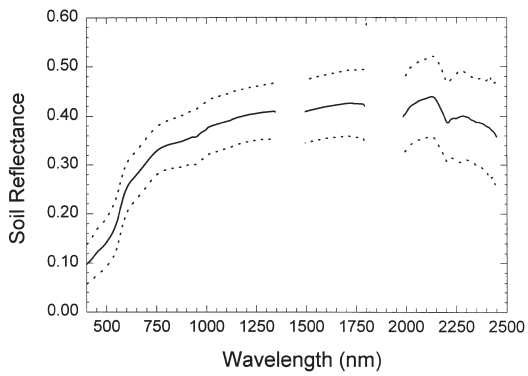

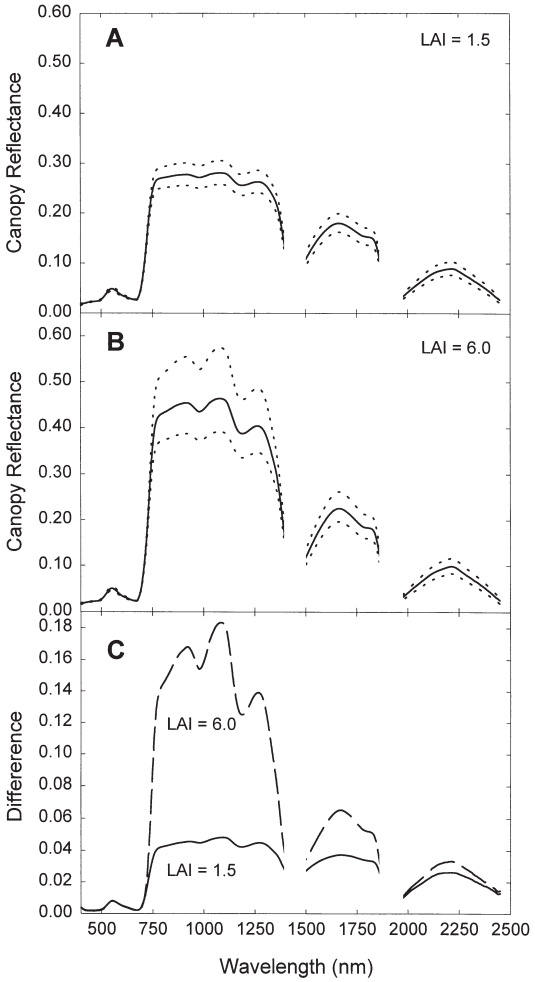

Figure 4. Effects of leaf optical variability (4 s.d. from Fig. 1) on nadir-viewed canopy reflectance as simulated for two hypothetical LAI scenarios. Mean leaf angle=45°. A) Canopy LAI=1.5; B) canopy LAI=6.0; C) high reflectance–low reflectance in panels A and B show that leaf optical variability has the largest effect on canopy reflectance in the NIR.

leaves), and enhances canopy absorption in "dark" regions (e.g., 680 nm for green leaves). Increases in LAI diminished in importance as canopy LAI increased, a result that has been widely reported previously (e.g., Asrar et al., 1984; Goward and Huemmrich, 1992; van Leeuwen and Huete, 1996; Asner and Wessman, 1997). The SWIR region was moderately responsive to LAI increases, falling between the VIS and NIR in overall sensitivity.

There was also an obvious deepening of the two water absorption features within the NIR (~1000 nm and 1200 nm) as LAI increased. While the overall NIR trend was toward increased scattering with increased leaf area (Fig. 5a), these NIR plateau absorption features "lagged" behind the rest of the plateau due to enhanced water absorption as canopy biomass increased. Analysis of first derivatives supports this conclusion, as the slope of the reflectance continuum near 1000 nm and 1200 nm increased as LAI increased (Fig. 5b). Other derivative results indicate the following regions to be highly sensitive to changes in canopy LAI: 1) the 695–700 nm region (the red edge), 2) the 1275–1350 nm region, and 3) the SWIR1. While the VIS and SWIR2 were somewhat sensitive to increases in LAI from 0.5 to 1.0, both lost further sensitivity at higher LAI values.

Leaf single-scattering albedo (ω) is a summary metric of leaf optical properties since it combines reflectance and transmittance at any given wavelength into a single value. From Figure 1, ω of green foliage is highest in the NIR, moderate in the SWIR, and lowest in the VIS ($\omega_{NIR}>\omega_{SWIR}>\omega_{VIS}$). ω can be plotted against modeled canopy reflectance values to determine under which structural scenarios, and at which wavelengths, leaf-level information is most directly represented at canopy scales. For a hypothetical vegetation cover comprised only of leaf material, high LAI canopies translate the most leaf-level information to the canopy scale (Fig. 6a). Leaf ω's in the 8–16% (found near 680 nm, Fig. 1) and 80–100% range (found in the NIR, Fig. 1) were most readily trans-

Figure 6. Relationship between leaf single scattering albedo (ω=reflectance+transmittance) and canopy reflectance with A) changing LAI and B) changing mean leaf angle of an ellipsoidal distribution. The best translation of leaf optical properties to the canopy level occurred when ω>90%, corresponding to the NIR plateau in Figure 5.

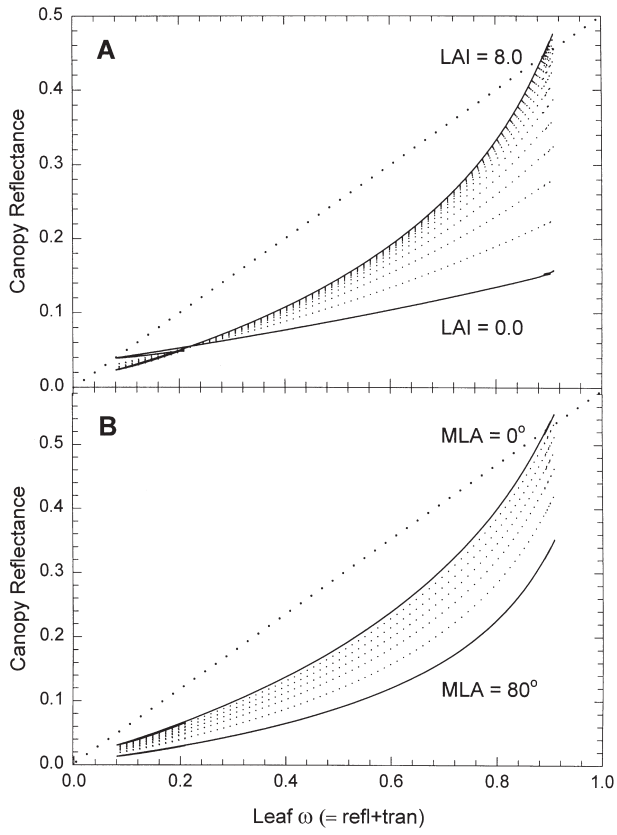

Table 2. Species Represented in the Tissue Optical Properties Analysis from Seven Edaphically and Climatically Diverse Ecosystems in North and South America

Species[a]	*Site*[b]	*Attributes*[c]	*Species*[a]	*Site*[b]	*Attributes*[c]
*Acacia berlandieri**	3	W,C3,L,D	*Miconia albicans*	7	W,C3,EG,AI
*Acacia farnesiana**	3	W,C3,L,D	*Miconia falax*	7	W,C3,EG,AI
*Acacia greggii**	3	W,C3,L,D	*Miconia ferruginata*	7	W,C3,EG,S,AI
*Acacia rigidula**	3	W,C3,L,D	*Morus microphylla*	2	W,C3,D
Acer negundo	1,4	W,C3,D	*Neea theifera*	7	W,C3,D
Agropyron cristatum	2	H,C3	*Ouratea hexasperma*	7	W,C3,EG,S
Aristida capillacea	7	H,C4	*Palicourea coriacea*	7	W,C3,EG,S,AI
Aristida purpurea	1	H,C4	*Panicum decipens*	7	H,C4
Ascosmium dasycarpum	7	W,C3,L,EG	*Panicum maximum*	7	H,C4
Aspidosperma tomentosum	7	W,C3,D	*Paspalum* spp.	3	H,C4
Berberis trifoliolata	2	W,C3,EG	*Pisonia noxia*	7	W,C3,D
Blepharcalyx salicifoleus	7	W,C3,EG	*Plathymenia reticulata*	7	W,C3,L,N,D
Bothriochloa ischaemum	3	H,C4	*Populus augustifolia*	1,4	W,C3,D
*Bouteloua curtipendula**	2	H,C4	*Prosopis glandulosa*	1,2,3,5,6	W,C3,L,N,D
*Bouteloua eriopoda**	5,6	H,C4	*Prosopis sonora*	2	W,C3,L,D
*Bouteloua rigidiseta**	1	H,C4	*Qualea grandiflora*	7	W,C3,D,S,AI
Byrsonima crassa	7	W,C3,EG,S	*Qualea multiflora*	7	W,C3,D,AI
Caryocar brasiliense	7	W,C3,D	*Qualea parviflora*	7	W,C3,D,AI
Celtis reticulata	2	W,C3,D	*Quercus buckleyi*	1	W,C3,D
*Cenchrus ciliaris**	3,7	H,C4	*Quercus gambelii*	1,4	W,C3,D
Cercis canadensis	2	W,C3,L,D	*Quercus pungens*	2	W,C3,EG,S
Chloris pluriflora	3	H,C4	*Quercus virginiana*	2	W,C3,EG,S
Colubrina texensis	2	W,C3,D	*Rapanea guianensis*	7	W,C3,EG,S
Condalia hookeri	3	W,C3,D	*Roupala montana*	7	W,C3,EG,S
Connarus fulvus	7	W,C3	*Rhus aromatica*	4	W,C3
Dalbergia misculobium	7	W,C3,L,N,D	*Rhus microphylla**	2	W,C3
Didymopanax macrocarpum	7	W,C3,EG,S	*Schizachyrium scoparium*	2	H,C4
Diospyros texana	3	W,C3,D	*Schlerolobium paniculatum*	7	W,C3,L,EG
Enterolobium ellipticum	7	W,C3,L,D	*Sophora secundiflora*	2	W,C3,EG,S
*Erioneuron pilsoum**	2	H,C4	*Sorgastrum nutans**	2	H,C4
Erythroxylum suberosom	7	W,C3,EG,S	*Stipa leucotricha*	1	H,C3
Forestiera angustofolia	2	W,C3,D	*Stryphnodendron adstringens*	7	W,C3,L,D
*Hilaria belangeri**	2	H,C4	*Styrax ferrugineta*	7	W,C3,EG
Hymenea stigonocarpa	7	W,C3,L,D	*Trachypogon montufari*	7	H,C4
Kielmeyera coriacea	7	W,C3,D,S	*Tripsacum dactyloides*	2	H,C4
Larrea tridentata	5,6	W,C3,EG	*Ugnadia speciosa*	2	W,C3,D
Leucaena retusa	2	W,C3,L,D	*Vochysia elliptica*	7	W,C3,EG,S,AI
Lonicera albiflora	2	W,C3,D	*Vochysia thyrsoides*	7	W,C3,EG,S,AI
Mahonia trifoliolata	3	W,C3,EG,S	*Zanthoxylum fagara*	3	W,C3,EG-NS
Melinis minutiflora	7	H,C4			

[a] Some of the known functional attributes of each species are provided. $n=10$ per species unless an * indicates $n=5$.
[b] 1) Vernon, 2) Sonora, 3) La Copita, 4) Colorado Springs, 5) Sevilleta, 6) Jornada, 7) Cerrado.
[c] W=woody plant, H=herbaceous plant, D=deciduous, EG=evergreen, S=sclerophyll, L=legume, N=confirmed nitrogen fixer, Al=aluminum hyperaccumulator, C3=C_3 physiology, C4=C_4 physiology.

lated to the canopy level under conditions of changing LAI. However, in the VIS region, the dynamic range of leaf optical properties is extremely narrow (Asner et al., 1998b), leading to similar constraints at canopy scales. Thus, the relationship between leaf and canopy reflectance is not significantly sensitive to changes in canopy structure within the VIS region. However, the presence of NPV does strongly influence the VIS spectral features and will be discussed later.

In the NIR, leaf optical properties were most directly expressed at the canopy level when LAI was very high, but quickly diminished as LAI decreased (Fig. 6a). These results are in close agreement with those of Baret et al. (1994), who found that leaf reflectance of sugar beets was best translated to canopy scales in the NIR region. Similarly, Kupiec and Curran (1995) found that changes in leaf chemistry of slash pine were most directly resolved at the canopy level in the NIR.

Leaf optical properties, and thus the biochemistry of leaf material, are thus generally underrepresented at canopy scales unless LAI is quite high. However, high LAI canopies do allow the weak leaf-level biochemical information to be enhanced at the canopy scale via multiple-scattering (Baret et al., 1994). The NIR region, which has the strongest multiple-scattering in green foliage canopies (due to high ω of foliage in NIR), has the best potential for enhancement of the leaf-level signal.

The previous analyses did not account for potential

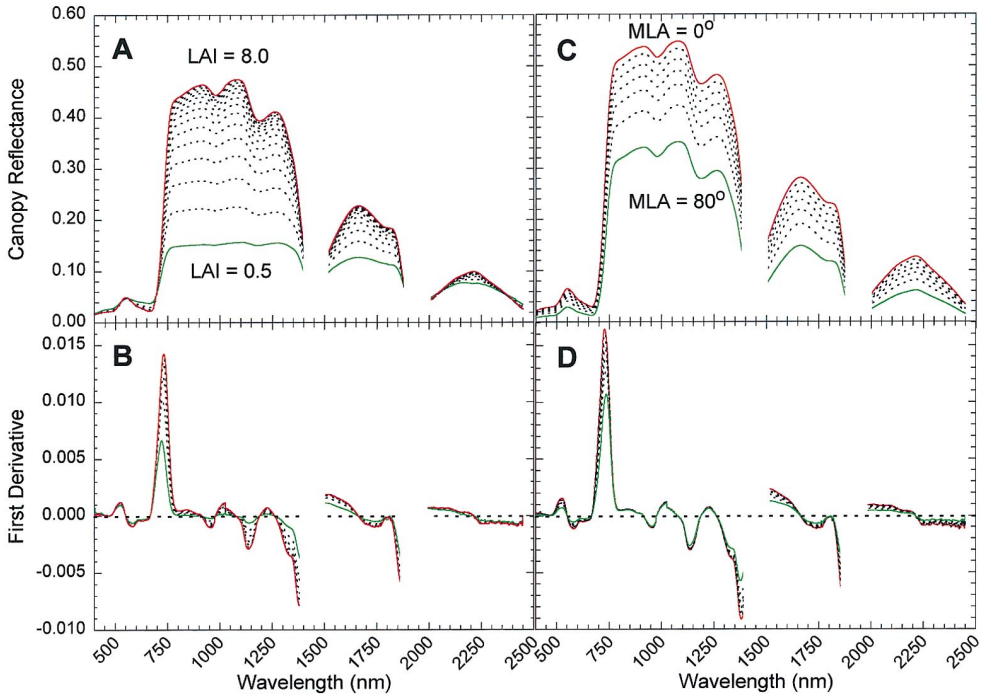

Figure 5. A) Effect of increasing LAI on canopy reflectance simulated with a mean leaf angle=45° and mean leaf optical properties from Figure 1. LAI was increased from 0.5 (green line) to 8.0 (red line). B) First derivative spectra coinciding with panel A. C) Effect of decreasing mean leaf angle (ellipsoidal distribution) on canopy reflectance, simulated with an LAI=5.0 and mean leaf optical properties from Figure 1. Mean leaf angle decreased from 80° (green line) to 0° (red line). D) First derivative spectra coinciding with panel C.

contributions to canopy reflectance resulting from variation in leaf angle distribution (LAD), which can be significant both within and between species (Table 5). The general effect of changing the mean leaf inclination angle of an ellipsoidal distribution is shown in Figure 5c (LAI=5.0). As mean leaf angle decreased from 80° to 0°, canopy reflectance increased in a similar manner to that observed with increasing LAI. However, closer inspection shows some important differences. First derivatives revealed that the shape of reflectance signal was sensitive to mean leaf angle changes in the following spectral regions: 1) the VIS to either side of the green peak at 550 nm, 2) the 695–700 nm red edge, and 3) the SWIR1 (Fig. 5d). Compared to LAI (Fig. 5a), leaf angle variation caused fewer changes to the shape of the reflectance signal (except for the red edge and SWIR1, where they were comparable). As mean leaf angle decreased, NIR reflectance increased as it did with increasing LAI, but the local water absorption features near 1000 nm and 1200 nm did not strengthen (Fig. 5d).

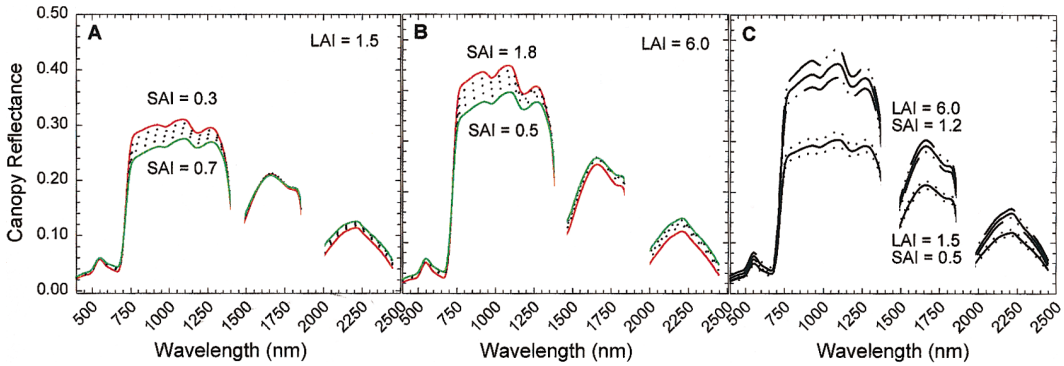

Figure 7. Effect of woody stem material on reflectance spectra of A) low LAI (1.5) and B) high LAI (6.0) canopies. Mean leaf and stem angles=45° and 75°, respectively. Stem area index was increased from 0.3–0.7 in low LAI case and 0.5–1.9 in the high LAI case. C) Variation in canopy reflectance due to observed variation in stem reflectance (from Fig. 2).

Table 5. Mean Leaf Angle for Dominant Species across a Wide Range of Ecosystems[a]

Vegetation Type	*Dominant Species*	*Mean Leaf Angle (°)*[b]	*Source*
Broadleaf evergreen montane forest	*Nothofagus solandri*	17 (14) 22 (15) 43 (22)	Hollinger (1989)
Desert scrub	*Prosopis glandulosa*	41–48	Asner (unpub.)
Desert shrubland	*Larrea tridentata*	33–71	Neufeld et al. (1988)
Desert shrubland-steppe	4 *Larrea* spp.	16–89	Ezcurra et al. (1991)
Moist tropical grassland/pasture	*Brachyaria* spp.	49–67	Asner and Townsend (unpub.)
Tropical moist forest	*Ocotea, heteropteris* spp., many others	5–60	Medina et al. (1978)
Subtropical savanna grasses	*Aristida, Stipa, Bouteloua* spp.	48–57	Asner et al. (in press)
Subtropical savanna trees	*Prosopis glandulosa*	37–45 49–79[a]	Asner et al. (in press)
Temperate coniferous forest	*Picea sitchensis*	10–50 (young needles) 25–65 (old needles)	Norman and Jarvis (1974)
Temperate deciduous forest	*Quercus* and *Acer* spp.	13–19 (subcanopy) 18–55 (overstory) 78[a]	Hutchison et al. (1986)
Temperate deciduous woodland	*Castanea sativa*	15–37	Ford and Newbould (1971)
Temperate mixed forest	*Pseudopanax crassifolius*	19–70	Clearwater and Gould (1955)
Temperate grassland	*Andropogon* spp., *Sorghastrum nutans*, others	45–60	Sellers and Hall (1992) Privette et al. (1996)
Temperate prairie grassland	*Silphium terebinthinaceum* (forb)	60	Smith and Ullberg (1989)
Tropical woodland	*Vochysia, Qualea, Miconia* spp., many others	24–78 68–86[a]	Asner et al. (unpub.)

[a] Mean stem angle is also provided when available.
[b] Parentheses indicate 1 standard deviation.

These results should be considered with caution for two reasons. First, the canopy simulation shown in Figures 5c,d used an LAI=5.0. For lower LAI canopies (<1.5), changing leaf angle distribution does not manifest in large first derivative changes in the VIS or SWIR regions, yet confounding factors soil background reflectance and NPV do play an important role (data not shown). Second, under actual remote sensing conditions, small slope changes in the VIS and SWIR regions are difficult to resolve due to instrument sensitivity (signal-to-noise ratio) and atmospheric contamination of the signal. Nonetheless, both AVIRIS signal-to-noise and methods for atmospheric correction have improved dramatically during the past several years, possibly making way for such analyses (Gao et al., 1993; Smith and Curran, 1996; Curran et al., 1997).

Leaf orientation had a strong effect on the expression of leaf optical properties at canopy scales (Fig. 6b). Similar to the LAI analysis (Fig. 6a), leaf scattering characteristics were best translated to the canopy level in the NIR (where ω=0.90). When foliage was oriented toward horizontal, leaf-level optical information was more directly resolved at canopy scales. The first scattering event (single scattering), which is enhanced at the top of the canopy when leaves are more horizontal, tends to be a very strong component of the bidirectional reflectance behavior of vegetation canopies (Myneni et al., 1989). Departure from horizontally oriented leaves resulted in the decreased expression of leaf optical properties at the canopy level, as single and multiple scattering allowed photons to travel farther down into the canopy, leading to greater signal attenuation. In canopies comprised of woody material, more vertically oriented foliage allows photons to interact with NPV and soil, thus introducing other biochemical (from woody stem and litter) and geochemical (from soil) information into the radiation field. The analyses presented in Figures 5 and 6 did not take into account this potential information added to a reflectance spectrum due to these other materials.

NPV Variability at Canopy Scales

Figure 7 depicts the radiative contribution of woody stem material to tree and shrub canopies. Based on the few studies quantifying the ratio of leaf and stem area in woody plant canopies (Table 4), the proportion of stem area was varied within a moderate (1.5) and high (6.0) LAI canopy. In the high LAI scenario, the NPVAI:PAI (plant area index=LAI+NPVAI) ratio was taken from temperate forest ecosystems (0.09–0.33; Deblonde et al., 1994; 0.18, D. Pataki, pers. commun.). The low LAI scenario used a ratio from a subtropical savanna tree canopy (0.22–0.48; Asner et al., in press).

The contribution of stem surfaces to both low and high LAI canopy reflectance spectra were significant.

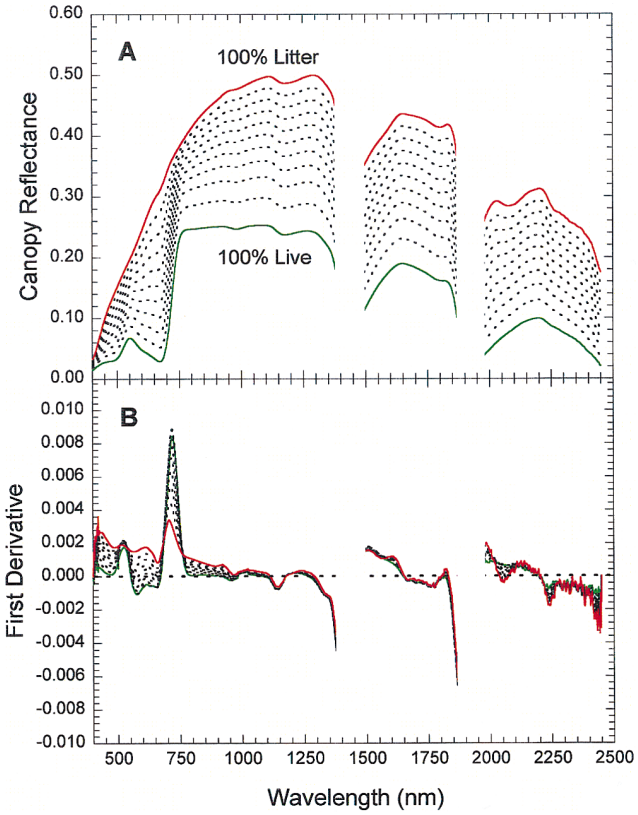

Figure 8. A) Changes in simulated canopy reflectance when the fraction of litter in a grassland canopy increases from 0% (green line) to 100% (red line). Total plant area index=2.0; mean leaf angle=60°; mean litter angle=45°; and mean grass leaf and litter optical properties from Figures 1 and 2. B) First derivative spectra coinciding with panel A.

Variation was highest in the NIR (5–9%) and lowest in the VIS (1–2%). Increases in the percentage of stem material in a canopy had the following effects: 1) Decreased the strength of the 680 nm absorption feature, 2) decreased the magnitude and increased the slope of the NIR plateau, 3) the entire SWIR region was elevated, and 4) the difference in the magnitudes of the NIR plateau (~1100 nm) and local SWIR maxima (1680 nm and 2200 nm) decreased. The effects of woody material are enhanced in the NIR because photons penetrate and exit the canopy more effectively in that spectral region, allowing maximum interaction of stem material in the radiation field. In the SWIR, stem effects are dampened (yet remain significant) by the strong water absorption features present in green foliage.

Stem optical variability played a smaller role in determining canopy reflectance (Fig. 7c) than did leaf optical properties (Fig. 4). In a canopy comprised of LAI=1.5 and SAI=0.5 (common in savanna trees; Asner et al., in press), stem properties caused maximum canopy reflectance variation of 3–4% in the NIR, while leaf optical properties resulted in 4–5% canopy variability (Fig. 4). In the high LAI canopy, stem optical variability resulted in

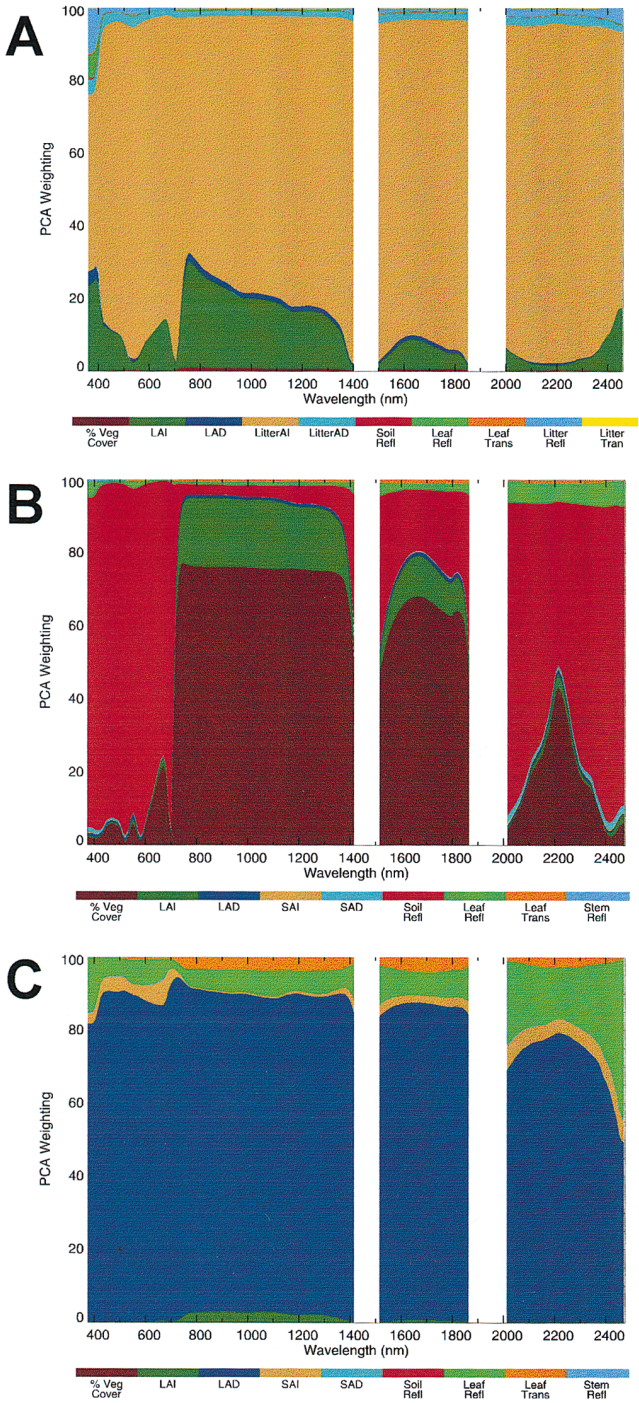

Figure 10. A) Perturbation analysis results for the Konza LTER grassland site. Height of each parameter at each wavelength shows its relative contribution to variability in canopy reflectance. LAI=leaf area index; LAD=leaf angle distribution; LitterAI=litter area index; LitterAD=litter angle distribution. B) Jornada LTER mesquite shrubland site. SAI=woody stem area index; SAD=woody stem angle distribution. C) Cerrado broadleaf woodland site.

5–6% canopy reflectance variation in the NIR, while leaf variability caused 14–18% variation. However, this modeling result also depends on the location of woody material

within the canopy (van Leeuwen and Huete, 1996). In these scenarios, the woody stems and foliage were assumed to be equally distributed (vertically) throughout the canopy. Stem optical variability will have more or less of an effect on canopy reflectance, depending on how much interaction woody material has with the photons that ultimately exit the canopy. The importance of material placement in the canopy remains unclear and is the focus of ongoing research.

Standing litter had a much larger impact on grass canopy reflectance than did woody material in arborescent canopies. Figure 8 shows the effect of increasing the relative proportion of standing litter (from 0 to 100%) in a grass canopy with plant area index (PAI)=2.0. As the relative abundance of litter increased, canopy reflectance increased significantly throughout the shortwave spectrum, with the largest changes in the NIR (16–26%) and SWIR1 (24–26%). The pigment absorption features (~450 nm and 680 nm) and NIR plateau observed in green canopies deteriorated as litter content increased. The red edge flattened and became a nearly linear reflectance continuum attribute. The features near 2075 nm and 2200 nm found in litter optical properties (Figure 2) emerged at the canopy level as well.

There were several distinct effects of standing litter on the first derivative spectra (Fig. 8b). First, the VIS region was highly sensitive to increases in canopy litter, particularly in the 550–700 nm range. This region was only moderately sensitive to changes in LAI (when LAI was low) and leaf angle (when LAI was relatively high) (Fig. 5); thus, the VIS range is a good candidate for assessing canopy litter content via first derivative spectra. The red edge (~695 nm) changed significantly with increasing litter as it did with changes in LAI and leaf angle. The SWIR2 region (2000–2100 nm and near 2250 nm) was also more than three times as sensitive to litter than to LAI or leaf angle variability (Fig. 8b).

Table 6. Canopy Structural Variables Used in AVIRIS Sensitivity Analyses of Three Ecosystems: Temperate Grassland at Konza LTER Site (Kansas), Arid Shrubland at Jornada LTER Site (New Mexico), and Broadleaf Tropical Woodland (Cerrado) in Brazil[a]

Parameters	*Konza Grassland*	*Jornada Shrubland*	*Cerrado Woodland*
Leaf area index	0.6–2.9[b]	0.9–3.9[e]	3.1–5.9[f]
Stem area index	—	0.4–0.6[e]	0.2–0.7[f]
Litter area index	10–60% of LAI[c]	—	—
Mean leaf angle	45–60°[d]	40–51°[e]	24–68°[f]
Mean stem angle	—	68–85°[e]	73–81°[f]
Mean litter angle	45–60°[d]	—	—
Vegetation cover	88–100%[c]	10–50%[e]	100%

[a] Value ranges taken from the sources referenced.
[b] Privette et al. (1996).
[c] Wessman et al. (1997).
[d] Sellers and Hall (1992).
[e] Asner and Wessman (unpub. data).
[f] Asner (unpub. data).

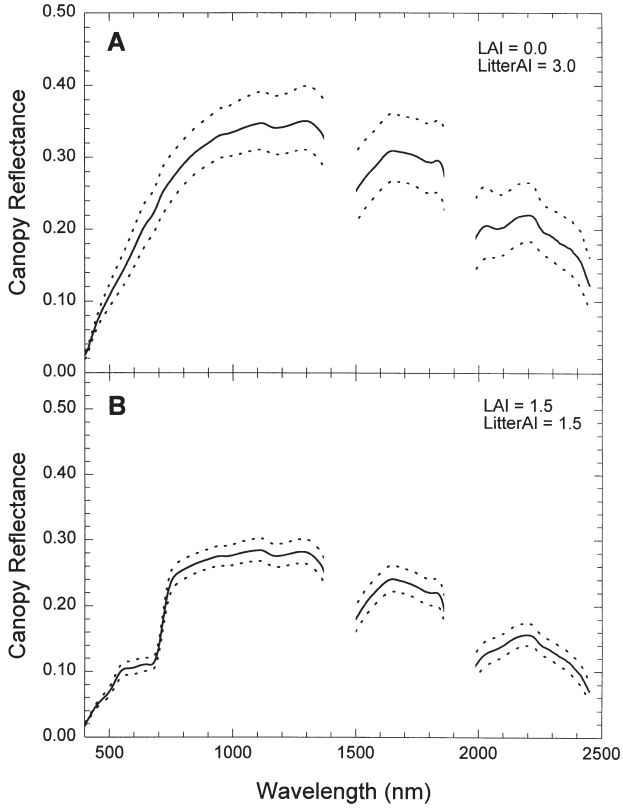

Figure 9. Role of litter optical variability at canopy scales for a grassland canopy with plant area index=3.0. A) 100% litter canopy (LAI=0.0, LitterAI=3.0) and B) 50% litter/ 50% live canopy (LAI=1.5, LitterAI=1.5).

Litter optical variability played an important role at the canopy level when the proportion of standing litter was high (Fig. 9a). Litter optics caused a maximum canopy-scale variation of 9% (absolute) in the SWIR1 when the canopy was completely senescent. In the VIS range, litter optical variability could account for 1–4% of the reflectance variation at the canopy level. The importance of litter optical variability was relatively small (2–4% in the SWIR1) when the canopy was only 50% senescent (Fig. 9b).

Variability in Contrasting Biomes

While the previous analyses help clarify the role of each scale-dependent factor contributing to a canopy reflectance spectrum, they do not necessarily incorporate the actual range of variation in plant characteristics that occurs within different ecosystems. More importantly, they do not provide a means to evaluate all of the factors simultaneously, and thus their relative importance cannot be assessed. The following sections reveal the relative role of the tissue optical, canopy structural, and soil reflectance properties driving the variation in landscape (pixel-level) reflectance signals in grassland, shrubland, and woodland biomes. The analysis employs the PCA approach de-

scribed earlier; parameter ranges are given in Table 6 for each ecosystem. Structural values were acquired from literature sources (Tables 4 and 5). The ranges of grassland leaf, litter, and soil properties were from the grassland portion of the North Texas (Vernon) site. Shrubland and woodland leaf, woody stem, and soil properties were from the Jornada and Cerrado sites, respectively.

Konza Grasslands

Perturbation analysis results for the Konza tallgrass prairie are shown in Figure 10a. Variability in surface reflectance was dominated by any presence of standing litter in the canopy. Specifically, litter area index played the most significant role (60–90% of the PCA variance), and was most important in the VIS (near 550 nm) and SWIR2 (near 2200 nm). LAI was the second most important factor (5–35% variance), peaking in importance in the NIR at roughly 720 nm. The optical properties of green (live) foliage and percent vegetation cover played a small role in driving surface reflectance variability (3–11% and 1–2%, respectively).

These results suggest that standing litter has a disproportionately strong effect on canopy reflectance in grasslands; a change in litter biomass plays a much stronger role in driving canopy reflectance variability than a concomitant change in LAI (or any other structural attribute). The very high single-scattering albedo of litter material (Fig. 2) is the source of this radiometric imbalance. This result has been observed in vegetation index data as well, as small increases in litter have a strong (usually nonlinear) effect on the NDVI (van Leeuwen and Huete, 1996).

Jornada Shrublands

The relative importance of leaf and canopy factors in the Jornada shrubland analysis (Fig. 10b) was sharply different from that of the Konza grassland. The primary determinants of canopy reflectance variability were vegetation cover and soil reflectance, with canopy LAI playing a secondary role. Foliar and woody stem optical properties contributed insignificantly to pixel-level reflectance variability, with the minor exception of the SWIR2 region, where leaf optical properties contributed 6–8% to the variation in reflectance.

Variation in vegetation cover and LAI dominated the surface reflectance signal in the NIR (75% and 23% of variance, respectively), with a decreasing role in the SWIR and VIS regions. Reciprocally, soil reflectance variability was the primary control over pixel reflectance in the VIS and SWIR2. Soil reflectance played a strong role in these spectral regions because it has a much higher single-scattering albedo (ω) than that of green foliage (Figs. 1 and 3).

In the VIS, the role of vegetation cover increased from roughly 3% at 575 nm to 21% at 680 nm. The significant decrease from the 680 nm peak to the local minima at 590 nm and 700 nm demonstrates that the strong chlorophyll absorption feature (at 680 nm) is expressed at the pixel level in shrublands as changes in vegetation cover occur, although this spectral region is dominated by the variability in soil reflectance. In this shrubland analysis, the range of soil reflectance values was taken directly from the Jornada site; thus the variability in this parameter is within the limits observed for that ecosystem. The dominant role of soil reflectance variability in arid ecosystems, such as the Jornada shrublands, has been widely recognized in other studies as well (e.g., Huete, 1988; Asrar et al., 1992; van Leeuwen et al., 1997). However, the results presented here suggest that the contribution of soil variation in arid lands can be quantified, possibly minimizing their effect on vegetation reflectance data. Further research is needed to determine which possibilities are viable.

Cerrado Woodlands

In the woodland analysis, LAI ranged from 3.1 to 5.9, SAI (stem area index) from 0.2 to 0.7, and mean leaf angle from 24° to 68°. These parameter ranges were derived from 30 common species found at the Cerrado site (Tables 2, 4, and 5; Asner, unpub. data). These LAI and mean leaf angle values are also typical of many other tropical and temperate woodland ecosystems (Tables 4 and 5). Foliar and woody stem optical properties and soil reflectance were permitted to vary within their observed range from the Cerrado portion of the data set (Figs. 1–3). To simplify the analysis, it was assumed that no canopy gaps were present (e.g., tree falls), which is not typically true in many woodland ecosystems (discussed later).

Figure 10c indicates that variation in canopy reflectance was primarily driven by leaf angle variability, with a secondary contribution from foliar optical properties. LAI variability had a negligible effect except in the NIR, where its contribution was only 3–5%. Leaf angle variability had the greatest effect in the VIS (82–89%) and NIR (88–93%). Foliar optical properties were important throughout the shortwave spectrum, but had the lowest impact at 700 nm (the red edge; 8% of variance) and the highest in the SWIR2 (22–54%). SAI played a small role in the VIS (5–7%) and in the SWIR2 (4–5%).

Leaf angle variation plays an important role in determining the reflectance of woodland canopies since the optical depth of a canopy with large amounts of foliage (high LAI) is also dependent on the orientation of the scatterers (leaves). More vertically oriented foliage allows photons to travel as both uncollided and scattered radiation down into the canopy. While increased interaction of photons with foliage may occur (gaining more of the foliage biochemical contribution to the signal), attenuation also increases. It is argued that woodland ecosystems are good candidates for analysis of foliar and canopy chemistry using imaging spectrometry because the canopy is closed and optically thick (e.g., Wessman et al., 1988; Martin and Aber, 1997). Whether the former assumption is true or not depends on the ecosystem in question. The

latter assumption is highly dependent on foliage density (related to LAI and gap fraction) and orientation.

Studies indicate that canopy gaps resulting from tree spacing, blowdowns, tree mortality, land use, and other factors are quite common and spatially variable in woodland ecosystems (e.g., Canham et al., 1990; Denslow and Spies, 1990; Young, 1995). Gaps expose litter, woody stem material, and bare soils to nadir-looking remote sensing instruments, and thus could violate the closed-canopy assumption. However, larger canopy gaps which expose the most NPV and soil will be limited to specific pixels when using an instrument with high spatial resolution such as AVIRIS. With coarse spatial resolution instruments, large gaps can significantly affect the remotely sensed signal. In fact, detection of this attribute has been a focus of several forest remote sensing studies using multiview angle data which is sensitive to gap fraction (Li and Strahler, 1985; Wu and Strahler, 1994; Li et al., 1995).

The assumption of an optically thick canopy is also wavelength-dependent. For example, photons in the visible region are attenuated more quickly than in the NIR. It follows that the relative importance of canopy structural and leaf biochemical properties in determining canopy reflectance will vary by wavelength. If the canopy is optically thick at a given wavelength, then the transfer of leaf optical properties (and potentially leaf chemistry) will be maximized for that wavelength (Fig. 6).

Efforts to estimate forest canopy chemistry with imaging spectrometry require an understanding of the variation, in both space and time, of foliage orientation (as well as LAI and gap fraction). To assume that leaf angle distributions do not vary within or between species across a landscape may be incorrect as several studies have shown species-specific foliar orientation (Table 5). Studies indicating relationships between species and foliar chemistry may, in fact, be sensitive to leaf angle distribution. However, Curran et al. (1997) studied the relationship between canopy chemistry and AVIRIS reflectance data in a monospecific slash pine stand, finding some of the most significant relationships ever reported. In that case, variation in leaf angle distribution was probably minimized (same species), allowing variation in foliar chemistry to translate most effectively to canopy-level reflectance. Had the leaf angle distribution parameter been constrained to a tighter range (e.g., 40–50° instead of 24–78°) in the Cerrado analysis, the relative contribution of leaf optical properties to canopy-level reflectance would have increased (e.g., from about 20–25% to 60–75% in the SWIR2; analyses not shown). However, the relative importance of LAI variability also would have increased (e.g., from 3–5% to 30–40% in the NIR).

CONCLUSIONS

Quantification of the scale-dependent nature of each tissue and structural attribute affecting canopy and landscape reflectance provides both an avenue to improve the interpretation of remotely sensed data and information to aid the development of new algorithms and technologies. Due to the structural and biochemical complexity of ecosystems, analyses based solely on field studies tend to be locationally and temporally dependent. In the case of radiation studies, field observations alone cannot resolve issues like those raised in this article. Conversely, studies relying upon modeling alone can be misleading, even inaccurate, if the ecologically realistic limits of each modeled variable are not known. Understanding the bounds on each variable within different ecosystems is required since the modeling results can differ drastically depending on the range of the values employed.

This study combined field observations with radiative transfer modeling to uncover the factors influencing the shortwave reflectance signal of three contrasting vegetation types. Evidence from the analyses presented in this article indicate the following:

- Variability in tissue optical properties is wavelength-dependent. For green leaves, the smallest variation is in the VIS region, while the largest is in the NIR. For standing litter material, minimum variation occurs in the VIS/NIR, while the largest variability is observed in the SWIR. Woody stem material shows opposite trends, with lowest variation in the SWIR and highest in the NIR.
- Variation in canopy structure (e.g., LAI and leaf angle) is significant, both within individual species and across landscapes, and this variability is the dominant control on canopy reflectance data (with the exception of soil reflectance and vegetation cover in sparse canopies such as shrublands).
- Leaf optical properties (and thus foliar chemistry) are expressed most directly at the canopy level within the NIR spectral region. However, LAI and leaf angle control the strength of this link.
- Stem material plays a small but significant role in determining canopy reflectance in woody plant canopies, especially those with LAI<5.0. However, this is also dependent on the location of woody material within the canopy.
- Standing litter significantly affects the reflectance characteristics of grassland canopies. Small increases in the percentage of standing litter lead to disproportionately large changes in canopy reflectance. Variation in litter optical properties plays a secondary role to structural attributes (e.g., leaf and litter area index) in determining canopy reflectance.
- The capabilities of vegetation remote sensing are ecosystem dependent (e.g., grasslands, shrub-

lands, and woodlands); that is, the structural attributes of ecosystems determine the relative contribution of leaf, canopy, and landscape factors driving variation in a reflectance signal. In addition, the relative contribution of tissue (leaves, woody stems, and litter) and structural attributes of ecosystems to a shortwave signal varies by wavelength both between and within vegetation types.

The results presented here are idealistic in that only canopy-level reflectance was simulated without the added complexity of the atmosphere. If the influence of the atmosphere can be adequately removed, then the trends found here remain pertinent to the interpretation of canopy reflectance data. The effects of solar and viewing geometry [Eq. (1)] were also not addressed in this study, yet both play a critical role in determining the reflectance characteristics of vegetation (e.g., Goel, 1988; Gerstl 1990; Myneni and Asrar, 1993; Meyer et al., 1995). Scattering of photons by vegetation is highly anisotropic. While this anisotropy may be considered noise in some studies, it is the signal in many other research efforts (e.g., Deering et al., 1992; Li et al., 1995; Braswell et al., 1996; Privette et al., 1996; Asner et al., 1997).

From a theoretical perspective, the analyses and conclusions drawn in this article apply to any optical remote sensing instrument, but are particularly pertinent to imaging spectrometer data. Analysis of first derivatives cannot be accomplished using broadband instruments (e.g., Landsat TM). The results presented here demonstrate potential for using the continuum nature of a hyperspectral signal to deconvolve issues of canopy structure and chemistry. Similarly, imaging spectrometry offers a capability to measure the radiative characteristics of canopies via narrow absorption features, which are only partially approachable using broadband instruments (e.g., Hall et al., 1990). The combination of narrowband absorption features and reflectance continua provides a unique avenue for understanding changes in the biophysical and biochemical characteristics of ecosystems. However, the vegetation reflectance signal is the integrated outcome of a complex interaction of tissue chemical, canopy structural, and landscape organizational factors. Therefore, deconvolution of these factors requires an understanding of the sources of variance in reflectance data (which is ecosystem-dependent) as well as an adequate sampling (spectral, angular, and temporal) of the shortwave spectrum.

I thank S. Archer, M. Bustamante, G. Cardinot, C. Cody, S. Fuhlendorf, P. Rundel, A. Townsend, C. Wessman, S. Zitzer, and S. Zunker for their help in collecting field data. K. Heidebrecht, C. Wessman, W. van Leeuwen, M. Bauer, and an anonymous reviewer provided extremely helpful comments on the manuscript. I also appreciate the generous help provided by many people at the Texas A&M Vernon, Sonora, and La Copita Research and Extension Centers, the Sevilleta and Jornada LTER sites, and at the IBGE Cerrado research site in Brazil.

This work was supported by NASA Innovative Research Grant NAGW-4689, NASA Interdisciplinary Science Grant NAGW-2662, NSF Research Training Grant BIR-9413218, and the NASA Earth System Science Fellowship Program.

REFERENCES

Adams, J. B., Sabol, D. E., Kapos, V., et al. (1995), Classification of multispectral images based on fractions of endmembers: application to land-cover change in the Brazilian Amazon. *Remote Sens. Environ.* 52:137–154.

Asner, G. P., and Wessman, C. A. (1997), Scaling PAR absorption from the leaf to landscape level in spatially heterogeneous ecosystems. *Ecol. Mod.* 101:396–414.

Asner, G. P., Wessman, C. A., and Privette, J. L. (1997), Unmixing the directional reflectances of AVHRR sub-pixel landcovers. *IEEE Trans. Geosci. Remote Sens.* 35:868–878.

Asner, G. P., Braswell, B. H., Schimel, D. S., and Wessman, C. A. (1998a), Ecological research needs from multi-angle remote sensing data. *Remote Sens. Environ.* 63:155–165.

Asner, G. P., Wessman, C. A., Schimel, D. S., and Archer, S. (1998b), Variability in leaf and litter optical properties: implications for BRDF model inversions using AVHRR, MODIS, and MISR. *Remote Sens. Environ.* 63:243–257.

Asner, G. P., Wessman, C. A., and Archer, S. (in press), Scale dependence of PAR absorption in terrestrial ecosystems. *Ecol. Applic.*

Asrar, G., Fuchs, M., Kanemasu, E. T., and Yoshida, M. (1984), Estimating absorbed photosynthetic radiation and leaf area index from spectral reflectance in wheat. *Agron. J.* 76: 300–306.

Asrar, G., Myneni, R. B., and Choudhury, B. J. (1992), Spatial heterogeneity in vegetation canopies and remote sensing of absorbed photosynthetically active radiation: a modeling study. *Remote Sens. Environ.* 41:85–103.

Baret, F., Vanderbilt, V. C., Steven, M. D., and Jacquemoud, S. (1994), Use of spectral analogy to evaluate canopy reflectance sensitivity to leaf optical properties. *Remote Sens. Environ.* 48:253–260.

Bidlack, J. E., and Buxton, D. R. (1992), Content and deposition rates of cellulose, hemicellulose, and lignin during regrowth of forage grasses and legumes. *Can. J. Plant Sci.* 72:809–820.

Borel, C. C., and Gerstl, S. A. W. (1994), Nonlinear spectral mixing models for vegetative and soil surfaces. *Remote Sens. Environ.* 47:403–416.

Boyer, M., Miller, J., Belanger, M., Hare, E., and Wu, J. (1988), Senescence and spectral reflectance in leaves in Northern Pin Oak (*Quercus palustris* Muenchh.). *Remote Sens. Environ.* 25:71–87.

Braswell, B. H., Schimel, D. S., Privette, J. L., et al. (1996), Extracting ecological and biophysical information from AVHRR optical data: an integrated algorithm based on inverse modeling. *J. Geophys. Res.* 101:23,335–23,345.

Campbell, G. S. (1986), Extinction coefficients for radiation in plant canopies calculated using an ellipsoidal inclination angle distribution. *Agric. For. Meteorol.* 36:317–321.

Canham, C. D., Denslow, J. S., and Platt, W. J. (1990), Light regimes beneath closed canopies and tree-fall gaps in temperate and tropical forests. *Can. J. For Res.* 20:620–635.

Clearwater, M. J., and Gould, K. S. (1995), Leaf orientation and light interception by juvenile *Pseudopanax crassifolius* (Cunn.) C. Koch in a partially shaded forest environment. *Oecologia* 104:363–371.

Curran, P. J., Dungan, J. L., Macler, B. A., Plummer, S. E., and Peterson, D. L. (1992), Reflectance spectroscopy of fresh whole leaves for the estimation of chemical concentration. *Remote Sens. Environ.* 39:153–166.

Curran, P. J., Kupiec, J. A., and Smith, G. M. (1997), Remote sensing of biochemical composition of a slash pine canopy. *IEEE Trans. Geosci. Remote Sens.* 35:415–420.

Daugherty, C. S. T., Ranson, K. J., and Biehl, L. L. (1989), A new technique to measure the spectral properties of conifer needles. *Remote Sens. Environ.* 27:81–91.

Deblonde, G., Penner, M., and Royer, A. (1994), Measuring leaf area index with the Li-cor LAI-2000 in pine stands. *Ecology* 75:1507–1511.

Deering, D. W., Middleton, E. M., and Irons, J. R. (1992), Prairie grassland bidirectional reflectances measured by different instruments at the FIFE site. *J. Geophys. Res.* 97:18,887–18,898.

Denslow, J. S., and Spies, T. (1990), Canopy gaps in forest ecosystems: an introduction. *Can. J. For. Res.* 20:619–630.

Dufrene, E., and Breda, N. (1995), Estimation of deciduous forest leaf area index using direct and indirect methods. *Oecologia* 104:156–162.

Effland, M. J. (1977), Modified procedure to determine acid insoluble lignin in wood and pulp. *Tech. Assoc. Pulp Pap. Ind. J.* 60:143–144.

Eiten, G. (1972), The Cerrado vegetation of Brazil. *Bot. Rev.* 38:201–341.

Ellsworth, D. S., and Reich, P. B. (1993), Canopy structure and vertical patterns of photosynthesis and related leaf traits in a deciduous forest. *Oecologia* 96:169–178.

Ezcurra, E., Montana, C., and Arizaga, S. (1991), Architecture, light interception, and distribution of *Larrea* species in the Monte Desert. *Ecology* 72:23–34.

Ford, E. D., and Newbould, P. J. (1971), The leaf canopy of a coppiced deciduous woodland. *J. Ecol.* 59:843–862.

Fourty, Th., Baret, F., Jacquemoud, S., Schmuck, G., and Verdebout, J. (1996), Leaf optical properties with explicit description of its biochemical composition: direct and inverse problems. *Remote Sens. Environ.* 56:104–117.

Gamon, J. A., Field, C. B., Goulden, M. L., et al. (1995), Relationships between NDVI, canopy structure, and photosynthesis in three Californian vegetation types. *Ecol. Appl.* 5:28–41.

Gao, B.-C., and Goetz, A. F. H. (1995), Retrieval of equivalent water thickness and information related to biochemical components of vegetation canopies from AVIRIS data. *Remote Sens. Environ.* 52:155–162.

Gao, B.-C., Heidebrecht, K. B., and Goetz, A. F. H. (1993), Derivation of scaled surface reflectance from AVIRIS data. *Remote Sens. Environ.* 44:165–178.

Gates, D. M., Keegan, H. J., Schleter, J. C., and Wiedner, V. R. (1965), Spectral properties of plants. *Appl. Opt.* 4:11–20.

Gausman, H. W. (1982), Visible light reflectance, transmittance, and absorptance of differently pigmented cotton leaves. *Remote Sens. Environ.* 13:233–238.

Gerstl, S. A. W. (1990), Physics concepts of optical and radar reflectance signatures: a summary review. *Int. J. Remote Sens.* 11:1109–1117.

Goel, N. S. (1988), Models of vegetation canopy reflectance and their use in estimation of biophysical parameters from reflectance data. *Remote Sens. Rev.* 4:1–212.

Goward, S. N., and Huemmrich, K. F. (1992), Vegetation canopy PAR absorptance and the normalized difference vegetation index: an assessment using the SAIL model. *Remote Sens. Environ.* 39:119–140.

Hall, F. G., Huemmrich, K. F., and Goward, S. N. (1990), Use of narrow-based spectra to estimate the fraction of absorbed photosynthetically active radiation. *Remote Sens. Environ.* 32:47–54.

Hollinger, D. Y. (1989), Canopy organization and foliage photosynthetic capacity in a broad-leaved evergreen montane forest. *Funct. Ecol.* 3:53–62.

Honzak, M., Lucas, R. M., Amaral, I., Curran, P. J., Foody, G. M., and Amaral, S. (1996), Estimation of the leaf area index and total biomass of tropical regenerating forests: comparison of methodologies. In *Amazonian Deforestation and Climate* (J. H. C. Gash, C. A. Nobre, J. M. Roberts, and R. L. Victoria, Eds.), Institute of Hydrology, London, pp. 365–381.

Huemmrich, K. F., and Goward, S. N. (1997), Vegetation canopy PAR absorptance and NDVI: an assessment for ten tree species with the SAIL model. *Remote Sens. Environ.* 61: 254–269.

Huete, A. R. (1988), A soil-adjusted vegetation index (SAVI). *Remote Sens. Environ.* 25:295–309.

Hutchison, B. A., Matt, D. R., McMillen, R. T., Gross, L. J., Tajchman, S. J., and Norman, J. M. (1986), The architecture of a deciduous forest canopy in eastern Tennessee, U.S.A. *J. Ecol.* 74:635–646.

Irons, J. R., Campbell, G. S., and Norman, J. M. (1992), Prediction and measurement of soil bidirectional reflectance. *IEEE Trans. Geosci. Remote Sens.* 30:249–260.

Jacquemoud, S. (1993), Inversion of the PROSPECT+SAIL canopy reflectance model from AVIRIS equivalent spectra: theoretical study. *Remote Sens. Environ.* 44:281–292.

Jacquemoud, S., Baret, F., and Hanocq, J. F. (1992), Modeling spectral and bidirectional soil reflectance, *Remote Sens. Environ.* 41:123–132.

Jacquemoud, S., Baret, F., Andrieu, B., Danson, F. M., and Jaggard, K. (1995), Extraction of vegetation biophysical parameters by inversion of the PROSPECT+SAIL models on sugar beet canopy reflectance data. Application to TM and AVIRIS sensors. *Remote Sens. Environ.* 52:163–172.

Jacquemoud, S., Ustin, S. L., Verdebout, J., Schmuck, G., Andreoli, G., and Hosgood, B. (1996), Estimating leaf biochemistry using the PROSPECT leaf optical properties model. *Remote Sens. Environ.* 56:194–202.

Jordan, C. F. (1969), Derivation of leaf area index from quality of light on the forest floor. *Ecology* 50:663–666.

Jordan, C. F., and Uhl, C. (1978), Biomass of a terra firme forest of the Amazon Basin. *Oecologia Plantarum* 13:387–400.

Klinge, H., and Herrera, R. (1983), Phytomass structure of natural plant communities on spodosols in southern Venezuela: the tall Amazon Caatinga forest. *Vegetatio* 53:65–84.

Kupiec, J. A., and Curran, P. J. (1995), Decoupling effects of the canopy and foliar biochemicals in AVIRIS spectra. *Int. J. Remote Sens.* 16:1731–1739.

Kuusk, A. (1991), The hot spot effect in plant canopy reflectance. In *Photon–Vegetation Interactions: Applications in*

Optical Remote Sensing and Plant Ecology (R. B. Myneni and J. Ross, Eds.), Springer-Verlag, New York, pp. 9–44.

Li, X., and Strahler, A. H. (1985), Geometric-optical modeling of a coniferous forest canopy. *IEEE Trans. Geosci. Remote Sens.* 23:207–221.

Li, X., Strahler, A. H., and Woodcock, C. E. (1995), A hybrid geometric optical-radiative transfer approach for modeling albedo and directional reflectance of discontinuous canopies. *IEEE Trans. Geosci. Remote Sens.* 33:466–480.

Maas, S. J., and Dunlap, J. R. (1989), Reflectance, transmittance, and absorptance of light by normal, etiolated, and albino corn leaves. *Agron. J.* 81:105–110.

Mass, J. M., Vose, J. M., Swank, W. T., and Martinez-Yrizar, A. (1995), Seasonal changes of leaf area index (LAI) in a tropical deciduous forest in west Mexico. *For. Ecol. Manage.* 74:171–180.

Major, D. J., Schaalje, G. B., and Wiegand, C. (1992), Accuracy and sensitivity analyses of SAIL model-predicted reflectance of maize. *Remote Sens. Environ.* 41:61–73.

Martin, M. E., and Aber, J. D. (1997), High spectral resolution remote sensing of forest canopy lignin, nitrogen, and ecosystem processes. *Ecol. Appl.* 7:431–443.

McLeod, S. D., and Running, S. W. (1988), Comparing site quality indices and productivity in Ponderosa pine stands of western Montana. *Can. J. For. Res.* 18:346–352.

Medina, E., Sobrado, M., and Herrera, R. (1978), Significance of leaf orientation for leaf temperature in an Amazonian sclerophyll vegetation. *Radiat. Environ. Biophys.* 15:131–140.

Mesarch, M. A., Walter-Shea, E. A., Asner, G. P., and Middleton, E. M. (in review), A revised methodology for conifer needle spectral optical properties. *Remote Sens. Environ.*

Meyer, D., Verstraete, M., and Pinty, B. (1995), The effect of surface anisotropy and viewing geometry on the estimation of NDVI from AVHRR. *Remote Sens. Rev.* 12:3–27.

Middleton, E. M., Chan, S. S., Mesarch, M. A., and Walter-Shea, E. A. (1996), A revised methodology for spectral optical properties of conifer needles, *IGARSS 96 Dig.* 2:1005–1009.

Murray, I., and Williams, P. C. (1987), Chemical principles of near-infrared technology. In *Near-Infrared Technology in the Agricultural and Food Industries* (P. Williams and K. Norris, Eds.), American Association of Cereal Chemists, St. Paul, MN, pp. 17–34.

Myneni, R. B., and Asrar, G. (1993), Radiative transfer in three-dimensional atmosphere–vegetation media. *J. Quant. Spectrosc. Radiat. Transfer* 49:585–598.

Myneni, R. B., Ross, J., and Asrar, G. (1989), A review on the theory of photon transport in leaf canopies. *Agric. For. Meteorol.* 45:1–153.

Nel, M. E., and Wessman, C. A. (1993), Canopy transmittance models for estimating forest leaf area index. *Can. J. For. Res.* 23:2579–2586.

Neufeld, H. S., Meinzer, F. C., Wisdom, C. S., et al. (1988), Canopy architecture of *Larrea tridentata* (DC.) Cov., a desert shrub: foliage orientation and direct beam radiation interception. *Oecologia* 75:54–60.

Norman, J. M., and Jarvis, P. G. (1974), Photosynthesis in sitka spruce (*Picea sitchensis* (Bong.) Carr.). *J. Appl. Ecol.* 11: 375–398.

Privette, J. L., Myneni, R. B., Tucker, C. J., and Emery, W. J. (1994), Invertibility of a 1-D discrete ordinates canopy reflectance model. *Remote Sens. Environ.* 48:89–105.

Privette, J. L., Emery, W. J., and Schimel, D. S. (1996), Inversion of a vegetation reflectance model with NOAA AVHRR data. *Remote Sens. Environ.* 58:187–200.

Roberts, D. A., Smith, M. O., and Adams, J. B. (1993), Green vegetation, non-photosynthetic vegetation, and soils in AVIRIS data. *Remote Sens. Environ.* 44:255–269.

Ross, J. K. (1981), *The Radiation Regime and Architecture of Plant Stands,* Kluwer Boston, Hingham, MA.

Running, S. W., Peterson, D. L., Spanner, M. A., and Teuber, K. B. (1986), Remote sensing of coniferous forest leaf area. *Ecology* 67:273–276.

Saldarriaga, J. G. (1985), Forest succession in the Upper Rio Negro of Colombia and Venezuela, Ph.D. thesis, University of Tennessee, Knoxville.

Salisbury, F. B., and Ross, C. (1969), *Plant Physiology.* Wadsworth, Belmont, CA.

Sellers, P. J., and Hall, F. G. (1992), FIFE in 1992: results, scientific gains, and future research directions. *J. Geophys. Res.* 97:19,091–19,109.

Shippert, M. M., Walker, D. A., Auerbach, N. A., and Lewis, B. E. (1995), Biomass and leaf area index maps derived from SPOT images for Toolik Lake and Imnavait Creek areas, Alaska. *Polar Rec.* 31:147–154.

Smith, G. M., and Curran, P. J. (1996), The signal-to-noise ratio (SNR) required for the estimation of foliar biochemical concentrations. *Int. J. Remote Sens.* 17:1031–1058.

Smith, M., and Ullberg, D. (1989), Effect of leaf angle and orientation on photosynthesis and water relations in *Silphium terebinthinaceum. Am. J. Bot.* 76:1714–1719.

Sprent, J. I., Geoghegan, I. E., and James, E. K. (1996), Natural abundance of ^{15}N and ^{13}C in nodulated legumes and other plants in the Cerrado and neighboring regions of Brazil. *Oecologia* 105:440–453.

Stewart, G. R., Joly, C. A., and Smirnoff, N. (1992), Partitioning or inorganic nitrogen assimilation between the roots and shoots of Cerrado and forest trees of contrasting plant communities of Southeast Brasil. *Oecologia* 91:511–523.

TAPPI (1975), Water solubles in wood and pulp, Tech. Assoc. Pulp Paper Ind., Atlanta, GA.

TAPPI (1976), Alcohol–benzene and dichloromethane solubles in wood and pulp, Tech. Assoc. Pulp Paper Ind., Atlanta, GA.

Thomas, J. R., Namken, L. M., Oerther, G. F., and Brown, R. G. (1971), Estimating leaf water content by reflectance measurements. *Agron. J.* 63:845–847.

van Leeuwen, W. J. D., and Huete, A. R. (1996), Effects of standing litter on the biophysical interpretation of plant canopies with spectral indices. *Remote Sens. Environ.* 55:123–134.

van Leeuwen, W. J. D., Huete, A. R., Walthall, C. L., Prince, S. D., Begue, A., and Roujean, J. L. (1997), Deconvolution of remotely sensed spectral mixtures for retrieval of LAI, fAPAR and soil brightness. *J. Hydrol.* 188/189:697–724.

Verdebout, J., Jacquemoud, S., and Schmuck, G. (1994), Optical properties of leaves: modelling and experimental studies. In *Imaging Spectrometry—A Tool for Environmental Observations* (J. Hill and J. Megier, Eds.), Kluwer Academic, Dordrecht, The Netherlands, pp. 169–191.

Verhoef, W. (1984), Light scattering by leaf layers with application to canopy reflectance modeling: the SAIL model. *Remote Sens. Environ.* 16:125–141.

Walter-Shea, E. A., and Norman, J. M. (1991), Leaf optical

properties. In *Photon–Vegetation Interactions* (R. B. Myneni and J. Ross, Eds.), Springer-Verlag, Berlin, pp. 229–252.

Welles, J. M., and Norman, J. M. (1991), Instrument for indirect measurement of canopy architecture. *Agron. J.* 83:818–825.

Wessman, C. A. (1990), Evaluation of canopy biochemistry. In *Remote Sensing of Biosphere Functioning* (R. J. Hobbs and H. A. Mooney, Eds.), Springer-Verlag, New York, pp. 135–156.

Wessman, C. A., Aber, J. D., Peterson, D. L., and Melillo, J. M. (1988), Remote sensing of canopy chemistry and nitrogen cycling in temperate forest ecosystems. *Nature* 335:154–156.

Wessman, C. A., Aber, J. D., and Peterson, D. L. (1989), An evaluation of imaging spectrometry for estimating forest canopy chemistry. *Int. J. Remote Sens.* 10:1293–1316.

Wessman, C. A., Bateson, C. A. and Benning, T. L. (1997), Detecting fire and grazing patterns in tallgrass prairie using spectral mixture analysis. *Ecol. Appl.* 7:493–511.

Woolley, J. T. (1971), Reflectance and transmittance of light by leaves. *Plant Physiol.* 47:656–662.

Wu, Y., and Strahler, A. H. (1994), Remote estimation of crown size, stand density, and biomass on the Oregon transect. *Ecol. Appl.* 4:299–310.

Young, T. P. (1995), Landscape mosaics created by canopy gaps, forest edges, and bushland glades. *Selbyana* 16:127–140.